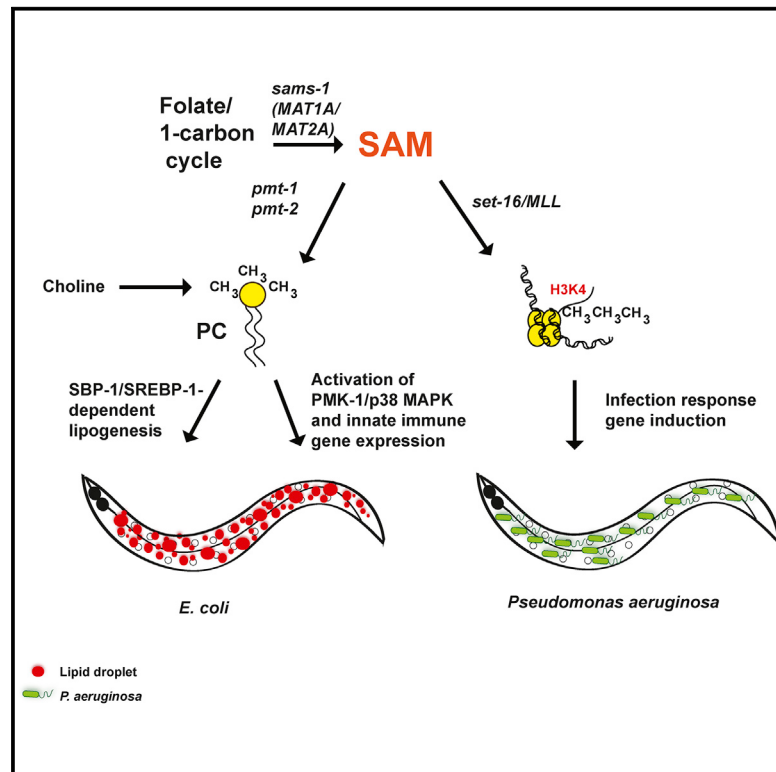


Cell Metabolism

s-Adenosylmethionine Levels Govern Innate Immunity through Distinct Methylation-Dependent Pathways

Graphical Abstract



Authors

Wei Ding, Lorissa J. Smulan, Nicole S. Hou, Stefan Taubert, Jennifer L. Watts, Amy K. Walker

Correspondence

amy.walker@umassmed.edu

In Brief

Methylation regulates diverse processes from transcription to phospholipid synthesis. Ding et al. find that methyl donor (SAM)-depleted *C. elegans* activate immune markers as methylation-dependent phospholipid synthesis decreases. However, the inability to methylate histones at immune gene promoters impairs survival on pathogens. Thus, SAM utilization varies with diet or stress conditions.

Highlights

- Immunity markers increase in SAM deficient *C. elegans* on a standard diet
- Immune activation is not protective because *Pseudomonas* rapidly kills *sams-1* animals
- *sams-1* animals fail to mount a transcriptional response to pathogens
- *sams-1* and *set-16/MLL* are critical for H3K4me3 in response to *Pseudomonas*

s-Adenosylmethionine Levels Govern Innate Immunity through Distinct Methylation-Dependent Pathways

Wei Ding,¹ Lorissa J. Smulan,¹ Nicole S. Hou,² Stefan Taubert,² Jennifer L. Watts,³ and Amy K. Walker^{1,*}

¹Program in Molecular Medicine, UMass Worcester, 373 Plantation Street, Worcester, MA 01605, USA

²Department of Medical Genetics, Centre for Molecular Medicine and Therapeutics (CMMT) and Child & Family Research Institute (CFRI), University of British Columbia (UBC), Vancouver, BC V5Z 4H4, Canada

³School of Molecular Biosciences, Washington State University, Pullman, WA 99164-6340, USA

*Correspondence: amy.walker@umassmed.edu

<http://dx.doi.org/10.1016/j.cmet.2015.07.013>

SUMMARY

s-adenosylmethionine (SAM) is the sole methyl donor modifying histones, nucleic acids, and phospholipids. Its fluctuation affects hepatic phosphatidylcholine (PC) synthesis or may be linked to variations in DNA or histone methylation. Physiologically, low SAM is associated with lipid accumulation, tissue injury, and immune responses in fatty liver disease. However, molecular connections among SAM limitation, methyltransferases, and disease-associated phenotypes are unclear. We find that low SAM can activate or attenuate *Caenorhabditis elegans* immune responses. Immune pathways are stimulated downstream of PC production on a non-pathogenic diet. In contrast, distinct SAM-dependent mechanisms limit survival on pathogenic *Pseudomonas aeruginosa*. *C. elegans* undertakes a broad transcriptional response to pathogens and we find that low SAM restricts H3K4me3 at *Pseudomonas*-responsive promoters, limiting their expression. Furthermore, this response depends on the H3K4 methyltransferase *set-16/MLL*. Thus, our studies provide molecular links between SAM and innate immune functions and suggest that SAM depletion may limit stress-induced gene expression.

INTRODUCTION

Metabolites can regulate signaling and transcriptional pathways by providing small molecules that modulate protein or nucleotide function, coordinating nutrition with physiology. For example, in *Caenorhabditis elegans*, dietary variation in vitamin B₁₂ leads to changes in fertility, lifespan, and gene expression, allowing adaptation to distinct nutritional sources (MacNeil et al., 2013; Watson et al., 2013; Watson et al., 2014). Another metabolite that can affect a broad array of mechanisms is s-adenosylmethionine (SAM). Produced by the 1-carbon cycle (1CC), SAM is the donor for methylation of histones and other proteins, nucleic acids, and is used in phospholipid synthesis (Kaelin and McKnight, 2013; Mato et al., 2008; Vance, 2014) (Figure 1A; see also Table S1 for human orthologs). Reduced 1CC function

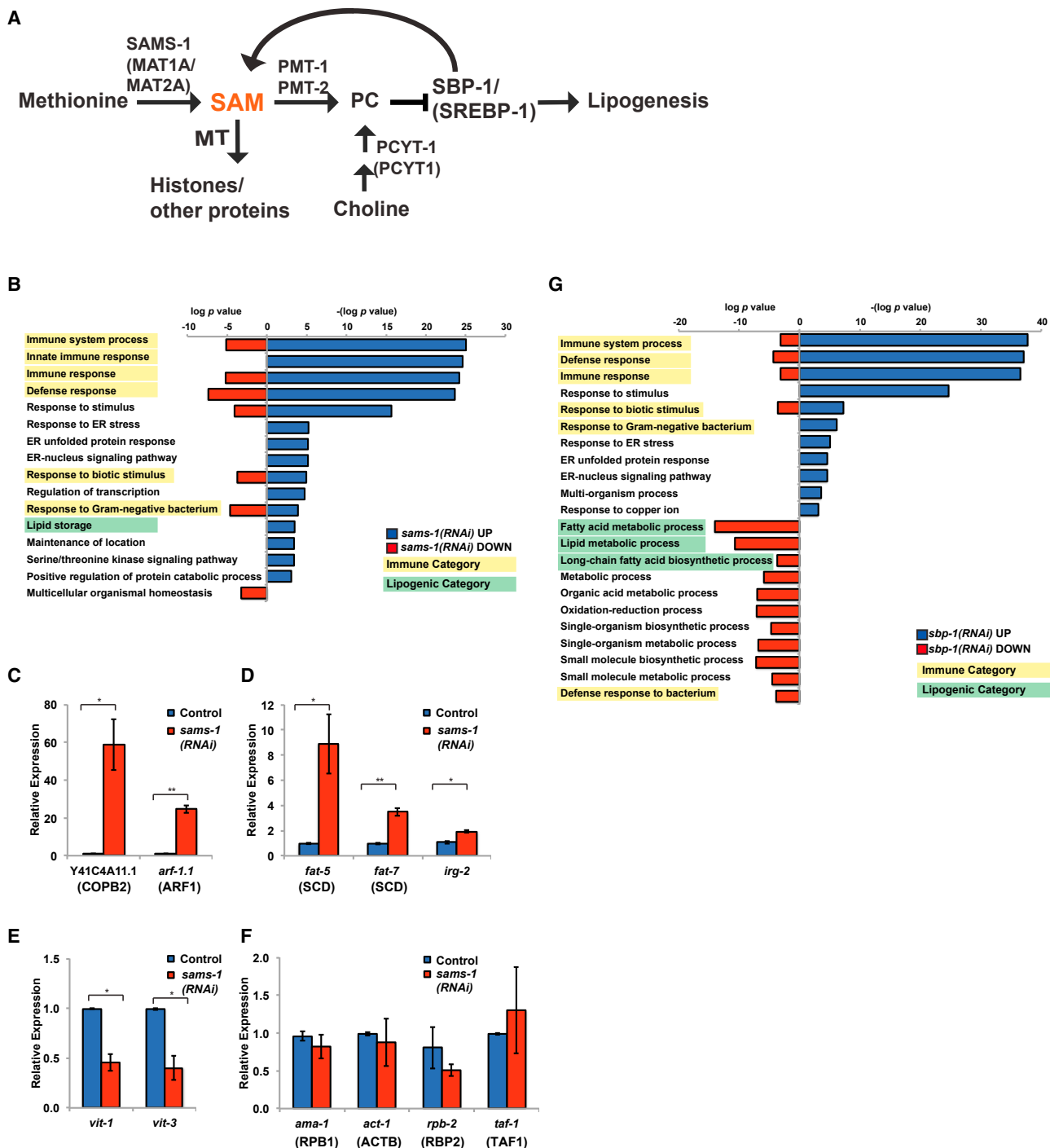
is strongly associated with metabolic disorders, particularly fatty liver disease, which is characterized by lipid accumulation and immune dysfunction (Lu et al., 2001). SAM deficiency may also underlie liver pathology in alcohol-induced fatty liver disease (ALD) and nutritional limitation of 1CC function accelerates injury in ALD models (Halsted et al., 2002). Mammalian cells have more than 200 genes predicted to encode SAM-dependent methyltransferases (Petrossian and Clarke, 2011). However, the mechanisms connecting SAM levels to specific methyltransferases and molecular changes underlying disease phenotypes are unresolved (Kaelin and McKnight, 2013).

We have previously used *C. elegans* to discern molecular mechanisms linking decreased SAM to lipogenesis and identified a conserved regulatory loop activating the transcription factor SBP-1/SREBP-1 when SAM or the methylated phospholipid phosphatidylcholine (PC) are low (Walker et al., 2011). Here, we find that *C. elegans* with reduced function of the SAM synthase *sams-1* and concomitant decreases in SAM also have complex immune phenotypes. *C. elegans* consuming standard *E. coli* diets have activated immune signatures linked to requirements for SAM in PC production. However, low SAM also affects histone methylation during acute transcriptional responses, limiting protective gene expression programs upon exposure to the bacterial pathogen *Pseudomonas aeruginosa*. Thus, phenotypic consequences of SAM deficiency differ as requirements for methylation are changed. Finally, our results suggest that low SAM restricts stress-responsive transcription, potentially linking 1CC dysfunction and tissue injury in metabolic disease.

RESULTS

sams-1 Knockdown Results in Activation of Innate Immune Genes in Absence of Pathogenic Bacteria

In *C. elegans*, knockdown of the SAM synthase *sams-1* decreases SAM and SAH levels around 65% and is associated with increased lipogenesis, decreased fertility, and extended lifespan (Hansen et al., 2005; Walker et al., 2011) (see also Figure S1A). We previously showed that lipogenic gene expression, lipid accumulation, and fertility defects in *sams-1* animals are linked to synthesis of PC, a methylated phospholipid. Reductions in PC lead to lipid accumulation by activating the transcription factor SBP-1/SREBP-1. To identify other groups of genes that change after *sams-1* RNAi and determine if they are also regulated by SBP-1/SREBP-1, we profiled whole genome mRNA expression from *sams-1* and *sbp-1* RNAi animals

**Figure 1. Co-regulation of Lipogenic and Immune Function Genes with Depletion of SAM**

(A) Schematic showing *C. elegans* pathways producing or utilizing SAM. MT is methyltransferase, SAM is s-adenosylmethionine, PC is phosphatidylcholine. Human names for orthologs are shown in parentheses, see also Table S1.

(B) Bar graphs comparing p values for GO categories of genes regulated more than 2.0-fold after *sams-1(RNAi)*. Downregulated genes are shown in red bars as log p value. To distinguish upregulated genes, -(log p value) was used for blue bars. Immune categories are highlighted in yellow, lipogenic in green. Genes are identified in Table S2, tab: GO Categories.

(C–F) Genes that were upregulated (C and D), downregulated (E) or not changed (F) in microarray studies were validated in qRT-PCR standardized to an exogenous “spike in” mRNA.

(G) Bar graphs comparing p values for GO categories of genes regulated more than 2.0-fold after *sbp-1(RNAi)*. Downregulated genes are shown in red bars as log p value. To distinguish upregulated genes, -(log p value) was used for blue bars. Immune categories are highlighted in yellow, lipogenic in green. Genes are identified in Table S3, tab: GO Categories.

(GEO: GSE70692). As expected, we found lipogenic genes increased in *sams-1(RNAi)* animals (Figure 1B, green labels; Table S2). Surprisingly, immune regulators were the most significantly enriched category of upregulated genes (Figure 1B, yellow labels; Table S2). These include components of mitogen activated protein kinase (MAPK) pathways, transcription factors important for immune gene activation as well as infection response genes, which encode antimicrobial effectors activated upon exposure to pathogens (see Table S2 tab: GO terms) (Engelmann et al., 2011). We validated expression profiling results by quantitative RT-PCR of selected genes normalized to *act-1* levels after *sams-1(RNAi)* (not shown), as well as in *sams-1(ok3033)* animals (Figures S1B and S1C). We also normalized qPCR validations to an external “spiked-in” RNA (JNK1a1 alpha, gift of Dr. Roger Davis). These results were similar to the microarray and to the *act-1* normalized qPCR for upregulated (Figures 1C and 1D), downregulated (Figure 1E), or unchanged genes (Figure 1F) tested. Finally, Lu et al. previously reported changes in some immunity-related genes in mice with a targeted deletion in the SAM synthase MAT1A and fatty liver disease (Lu et al., 2001). Taken together, these results suggest that upregulation of innate immune genes is a major response to methyl donor depletion.

We previously identified a feedback loop stimulating lipogenic SBP-1/SREBP-1-dependent gene expression in *sams-1(RNAi)* animals (Walker et al., 2011) (see also Figures 1B and 1G, green highlighting). Innate immune genes may be activated by SREBP proteins in mammalian macrophages (Im et al., 2011); therefore, we asked if SBP-1/SREBP-1 was required for immune gene expression after *sams-1* RNAi in *C. elegans*. However, these genes were also broadly upregulated after *sbp-1* RNAi (Figure 1G). Furthermore, activation of innate immune genes in *sams-1(lop)* animals occurs when *sbp-1* is depleted (not shown). Thus, innate immune gene upregulation in *sams-1* animals seems unlikely to depend on of feedback loops activating SBP-1/SREBP-1 and may be downstream of distinct SAM and/or PC-dependent pathways.

The PMK-1/p38 MAPK Kinase Pathway Is Constitutively Active in *sams-1* Animals

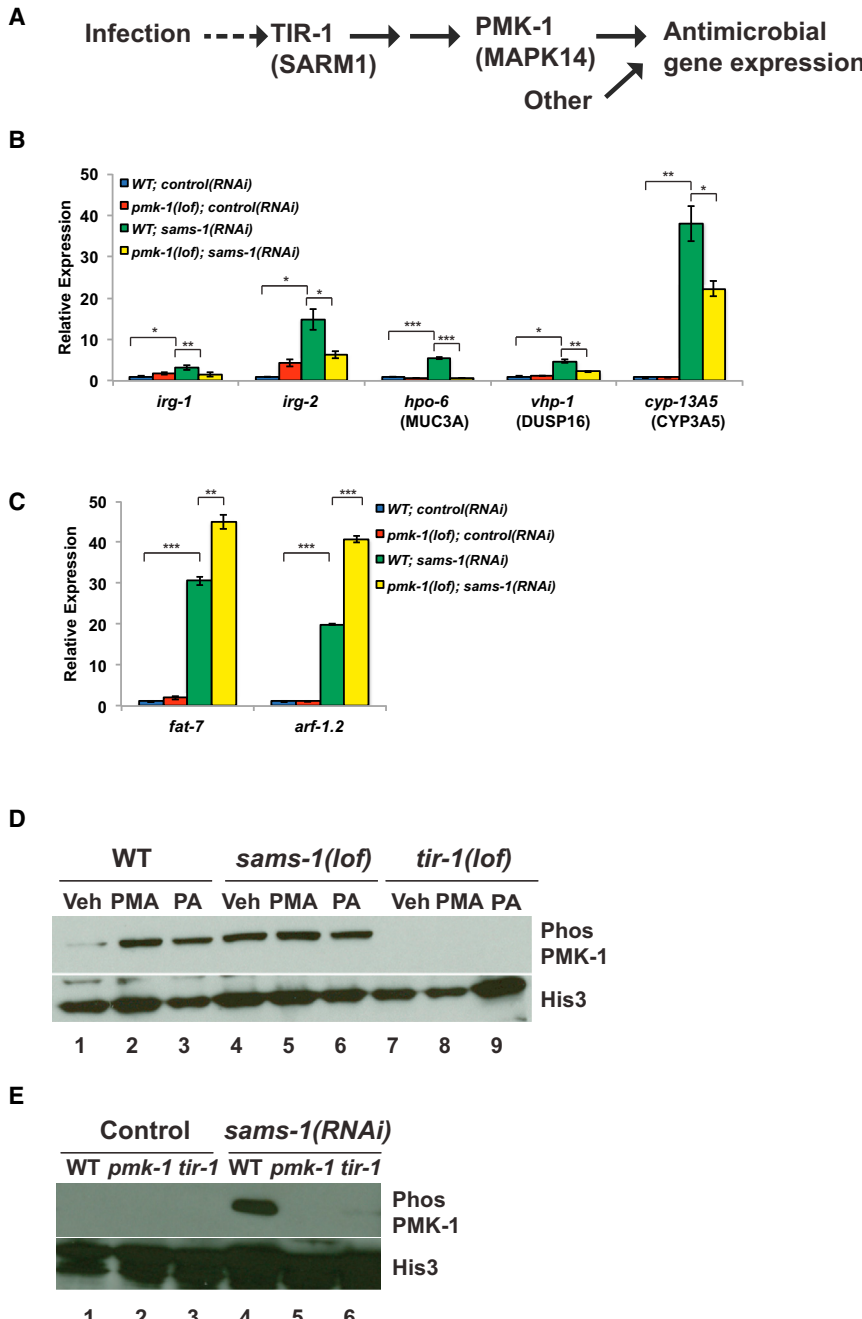
Innate immunity in *C. elegans* depends on PMK-1, a MAPK14/p38 MAP Kinase important for pathogen-responsive expression of many infection response genes (Kim, 2013; Troemel et al., 2006) (Figure 2A). Next, we asked if *sams-1*-dependent increases in immune gene expression required *pmk-1* and found that upregulation was less robust when *sams-1* was depleted in *pmk-1(lop)* mutants (Figure 2B). We also examined expression of *irg-1*, which is induced independently of *pmk-1* upon *Pseudomonas* exposure (Troemel et al., 2006). Although not identified in our microarray study, *irg-1* reproducibly increased after *sams-1* RNAi in qRT-PCR experiments, requiring *pmk-1* (Figure 2B). Thus, there may be some regulatory distinctions between low SAM and pathogen exposure. Loss of *pmk-1* did not limit upregulation of lipogenic genes, or *arf-1.1*, the gene with the highest-fold increase in *sams-1(RNAi)* microarrays (Figure 2C), demonstrating that *pmk-1* is not generally required for transcriptional changes in *sams-1(RNAi)* animals.

PMK-1 can be activated by various stresses; however, pathogen-responsive phosphorylation depends on a conserved

signal transduction pathway downstream of the TIR-1/SARM1 adaptor protein (Couillault et al., 2004; Kim et al., 2002; Troemel et al., 2006) (Figure 2A). To determine if innate immune gene activation was accompanied by PMK-1/p38 MAPK phosphorylation through this pathogen-response pathway, we determined levels of phosphorylated PMK-1/p38 in *sams-1(lop)* or RNAi animals (Figures 2D and 2E). As expected, PMK-1/p38 MAPK phosphorylation is induced in response to PMA (a stimulator of p38 MAPKs in *C. elegans* and mammals; Kawli and Tan, 2008) (Figure 2D, lanes 1 and 2) or upon exposure to *Pseudomonas* (Figure 2D, lanes 1 and 3) and fails to occur in animals lacking the upstream adaptor *tir-1* (Figure 2D, lanes 1–3 and 7–9). Strikingly, PMK-1/p38 MAPK was constitutively phosphorylated in *sams-1(lop)* animals (Figure 2D, lane 4) or after *sams-1* RNAi (Figure 2E, lane 4) and phosphorylation was refractory to additional stimulation with PMA or *Pseudomonas* (Figure 2D, lanes 4–6). Appearance of this band did not occur after *pmk-1* was also mutated (Figure 2E, lanes 4 and 5) and decreased when *tir-1* was absent (Figure 2E, lanes 4 and 6), suggesting that this PMK-1/p38 MAPK phosphorylation occurs in the context of pathogen-responsive signaling, even in the absence of bacterial stimuli.

Innate Immune Activation Is Downstream of PC in *sams-1* Animals

SAM has not been previously identified as an effector of PMK-1/p38 MAPK signaling. Therefore, we asked which methylation-dependent processes (Figure 1A) might link SAM to innate immune activation. To distinguish between PC-dependent or -independent effects, we provided dietary choline, which enables methylation-independent PC production (Vance, 2014), returns PC levels to wild-type levels (Figure S1D), and robustly rescues lipogenic phenotypes after *sams-1(RNAi)* (Walker et al., 2011). *C. elegans* lack a betaine hydroxymethyltransferase ortholog, making it unlikely that choline acts to regenerate SAM in nematodes (Wasmuth et al., 2008). First, we profiled genome-wide mRNA expression in *sams-1(RNAi)* and *sams-1(RNAi)* animals treated with choline (GEO: GSE70693). Choline had few significant effects on gene expression in control animals (Figure 3A, Vec/CH; Table S3). Surprisingly, most gene expression changes after *sams-1(RNAi)* were returned to wild-type levels by choline (Figure 3A). As in our previous array study (Figure 1B), we found that many lipogenic and innate immune genes were upregulated (Figures 3B and 3C; Figures S1B and S1C). Next, to determine if blocking PC synthesis downstream of SAM was necessary and sufficient to affect innate immune gene expression, we performed RNAi of the rate-limiting enzyme for PC production, *pcyt-1/PCYT1*. We found that *pcyt-1* RNAi was sufficient to activate lipogenic genes (as in (Walker et al., 2011)), innate immune genes (Figures S1E–S1J) and also induced PMK-1 phosphorylation (not shown). There was little significant change in the expression of lipogenic or immune genes in *sams-1(lop)*; *pcyt-1(RNAi)* animals, as would be expected if these *sams-1* and *pcyt-1* act in the same pathway. We noted that choline treatment caused increased expression of innate immune genes in wild-type animals exposed to *pcyt-1* RNAi. Importantly, choline was no longer sufficient to rescue gene expression increases in *sams-1(lop)*; *pcyt-1(RNAi)* animals, demonstrating that PC biosynthetic enzymes are required for choline rescue of *sams-1* immune phenotypes. Finally, we found that PMK-1/p38



MAPK phosphorylation returned to control levels in *sams-1(RNAi)* animals supplemented with choline (Figure 3E). Thus, mechanisms activating innate immunity in low SAM appear to be directly linked to PC production.

sams-1(lof) Animals Die Rapidly When Exposed to *Pseudomonas*

The presence of phosphorylated PMK-1 and increases in immune genes suggest that *sams-1* animals could resist pathogenic challenge. To test this, we exposed *sams-1(lof)* animals to virulent *Pseudomonas* (PA14). Surprisingly, *sams-1(lof)* ani-

Figure 2. Constitutive Activation of Innate Immune Pathway in after *sams-1* Depletion

(A) Schematic showing p38/PMK-1 mitogen-activated protein kinase signaling during response to bacterial infection in *C. elegans* (Kim, 2013).

(B) qRT-PCR comparing innate immune gene expression in *sams-1(lof)* and *pmk-1(lof); sams-1(lof)* mutants.

(C) qRT-PCR comparing expression of a lipogenic (*fat-7*) or other (*arf-1.1*) gene highly expressed gene in *sams-1(lof)* and *pmk-1(lof); sams-1(lof)* mutants.

(D) Immunoblot of phospho-PMK-1 in vehicle (Veh), phorbol acid treated (PMA) and *Pseudomonas aeruginosa* (PA) exposed wild-type (WT), *sams-1(lof)*, or *tir-1(lof)* mutants. Histone 3 shows loading.

(E) Wild-type, *pmk-1(lof)* or *tir-1(lof)* animals were exposed to control or *sams-1(RNAi)* and immunoblotted with antibodies to phospho-PMK-1 or Histone 3. Error bars show SD. Results from Student's t test shown by * <0.05 , ** <0.01 , *** <0.005 .

mals died faster than control animals on PA14 (Figure 4A; Table S4). Survival of *sams-1(lof); pmk-1(lof)* animals was identical to *pmk-1(lof)* alone. *Pseudomonas* represents a distinct nutritional source from *E. coli*; therefore, we asked if the bacterial food source or the strain virulence affected survival by exposure to the attenuated strain *Pseudomonas gacA* (Tan et al., 1999). In contrast to poor survival on PA14, we found that *sams-1(lof)* animals lived slightly longer than wild-type on *Pseudomonas gacA* and that *pmk-1* was important for this effect (Figure 4B; Table S4). This suggests that poor survival on PA14 is linked to pathogenicity rather nutritional content and that the constitutive phosphorylation of PMK-1 could play a role in *sams-1(lof)* animals in moderate or weakly pathogenic contexts. *sams-1(RNAi)* animals live longer than wild-type animals when fed *E. coli*; although this effect appears linked to dietary restriction, the mechanisms remain unclear (Hansen et al., 2005). Links between innate immunity and lifespan extension (Kurz and Tan, 2004) prompted

us to ask if *pmk-1* was also needed for lifespan extension of *sams-1(lof)* on *E. coli*. However, *pmk-1* was dispensable for this lifespan extension (Figure 4C), demonstrating that the control of lifespan in *sams-1* animals differ from effects on innate immunity.

Sensitivity to pathogens can arise from mechanisms including failure of the PMK-1/p38 MAP kinase pathway or clearance of intestinal bacteria via effects on defecation (Kim, 2013). The constitutive activation of PMK-1 (Figures 2D and 2E) in *sams-1* animals suggests that signaling to PMK-1 is intact, but insufficient for full protection. We also examined bacterial load in *sams-1(lof)* animals and found more *Pseudomonas* (PA14 GFP)

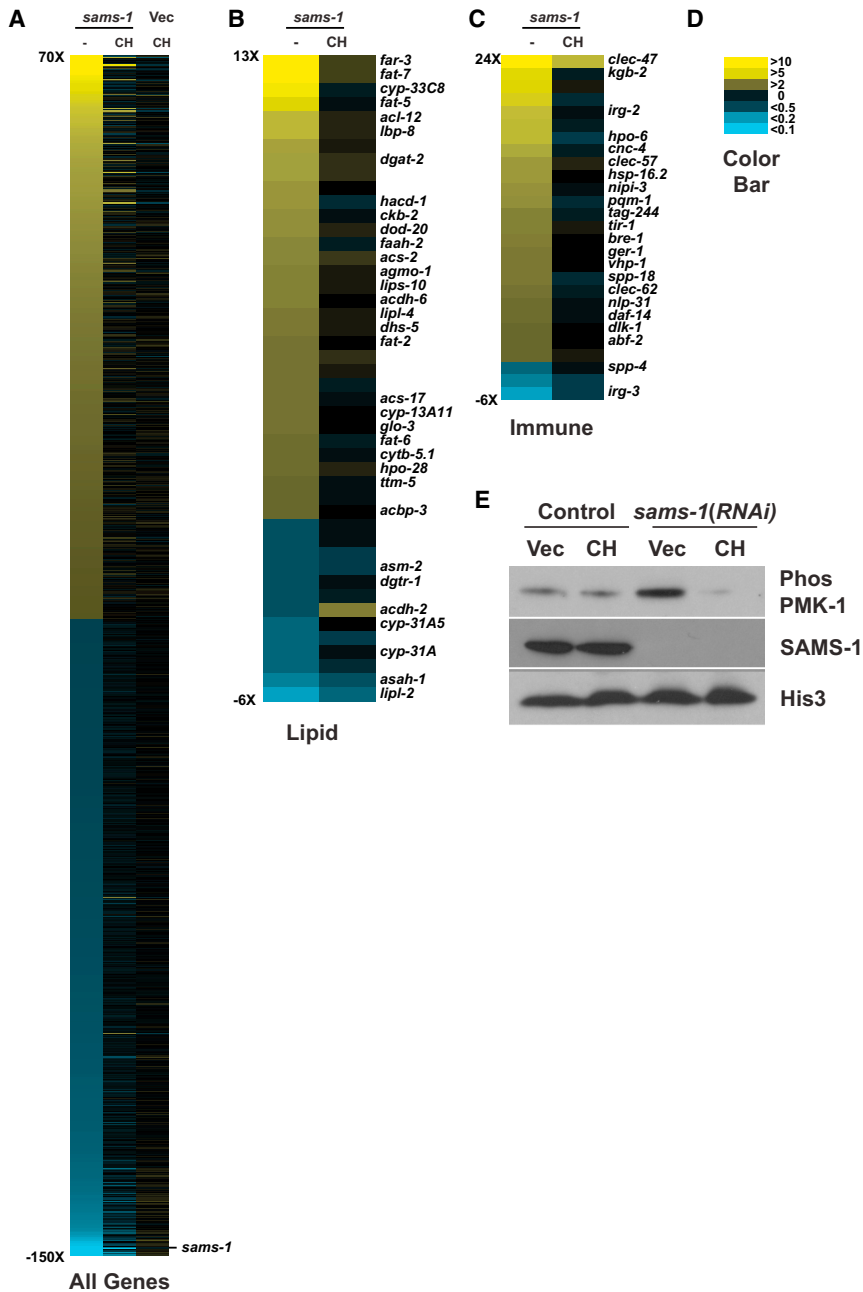


Figure 3. Restoration of PC Synthesis through Dietary Choline Rescues Innate Immune Phenotypes in sams-1(RNAi) Animals

(A) Heat map of genome-wide expression changes in *sams-1(RNAi)*, *sams-1(RNAi)* rescued by choline, or vector-only control (Vec) animals supplemented with choline.

(B–D) Heat map showing changes in expression level and choline rescue of lipogenic (B) and immune function (C) genes. Color values are shown in (D).

(E) Control (Vec) or *sams-1(RNAi)* animals which were grown on normal media or media supplemented with dietary choline (CH) were immunoblotted with antibodies recognizing phospho-PMK-1, SAMS-1, or Histone 3.

in the gut lumen after 24 or 48 hr with additional intestinal distension, another hallmark of *Pseudomonas* sensitivity (Irazoqui et al., 2010) (Figures 4D–4F). General mechanisms regulating bacterial processing were not grossly affected because *E. coli* (OP50 GFP) levels were similar in *sams-1(lf)* animals and wild-type (Figures 4E and 4F, not shown). Thus, mechanisms limiting survival of *sams-1(lf)* animals on *Pseudomonas* appear distinct from previously described pathogen responses.

Failure of Transcriptional Response to *Pseudomonas* in *sams-1(lf)* Animals

Despite activation of the protective PMK-1/p38 MAPK pathway, *sams-1(lf)* animals die rapidly on *Pseudomonas*. This paradox

suggests SAM-depleted animals are deficient in other aspects of the pathogen response. To understand what these impairments might be, we examined the transcriptional dynamics for the innate immune genes that increase in expression upon contact with *Pseudomonas*, referred to as infection response genes. Upon exposure to virulent *Pseudomonas*, wild-type *C. elegans* rapidly remodel gene expression, with some transcripts rising 200-fold within 4–8 hr (Troemel et al., 2006) (see also Figures 5A–5D). Although infection response genes are upregulated in *sams-1* animals fed *E. coli*, the increase is moderate (2–5 fold, with a few as high as 10-fold) (Figure 1B; Figure S1C). Remarkably, induction of these genes did not occur in *sams-1(lf)* animals exposed to virulent *Pseudomonas* (Figures 5A and 5B). This effect did not extend to genes specific to other stresses because the oxidative stress response gene, *sod-3*, remained unchanged. To determine if failure to induce these genes was linked to higher basal expression on *E. coli*, we examined *Pseudomonas*-responsive genes from Troemel et al. (2006) that were expressed normally in *sams-1* ani-

mals fed *E. coli*. We found these infection response genes also failed to increase in *sams-1(lf)* animals exposed to *Pseudomonas* (Figures 5C and 5D). Thus, the transcriptional response to *Pseudomonas* is blunted when SAM is depleted and suggests that a breakdown in stress-inducible gene expression underlies pathogen sensitivity in *sams-1(lf)* animals.

Moderate increases of innate immune genes after *sams-1(RNAi)* on *E. coli* appears linked to both SAM and PC, as dietary choline returns gene expression to wild-type levels (Figure 3C; Figure S1C). We next asked if induction defects were related directly to PC production or were instead due to deficiencies in other methylation-dependent processes. We differentiated SAM/PC and SAM PC-independent pathways using several

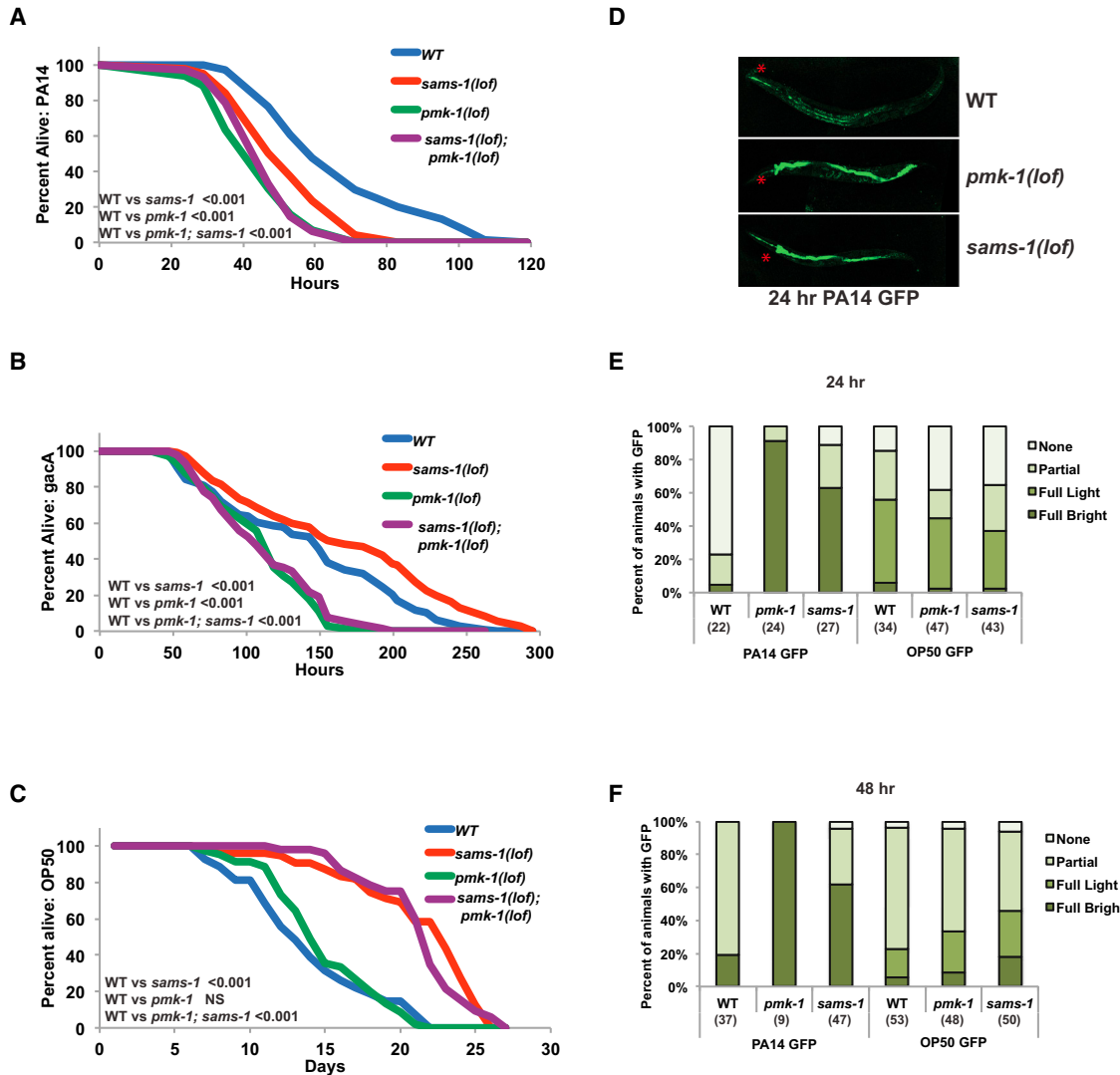


Figure 4. Reduced Resistance to *Pseudomonas aeruginosa* in *sams-1(lof)* Animals

(A–C) Representative Kaplan-Meir plot comparing survival of (WT), *sams-1(lof)*, *pmk-1(lof)* and *pmk-1(lof); sams-1(lof)* mutants exposed to pathogenic *Pseudomonas aeruginosa*, PA14 (A), the attenuated *Pseudomonas* strain *gacA* (B), or *E. coli* OP50 (C). NS is not significant. Additional statistics are available in Table S4. All strains in (A), (B), and (C) were raised on *cdc-25(RNAi)* to prevent egg laying.

(D) Fluorescent micrograph showing *Pseudomonas* load (PA14 GFP) after 24 hr exposure in intestines of wild-type, *pmk-1(lof)*, and *sams-1(lof)* mutants. Red asterisks show pharynx position.

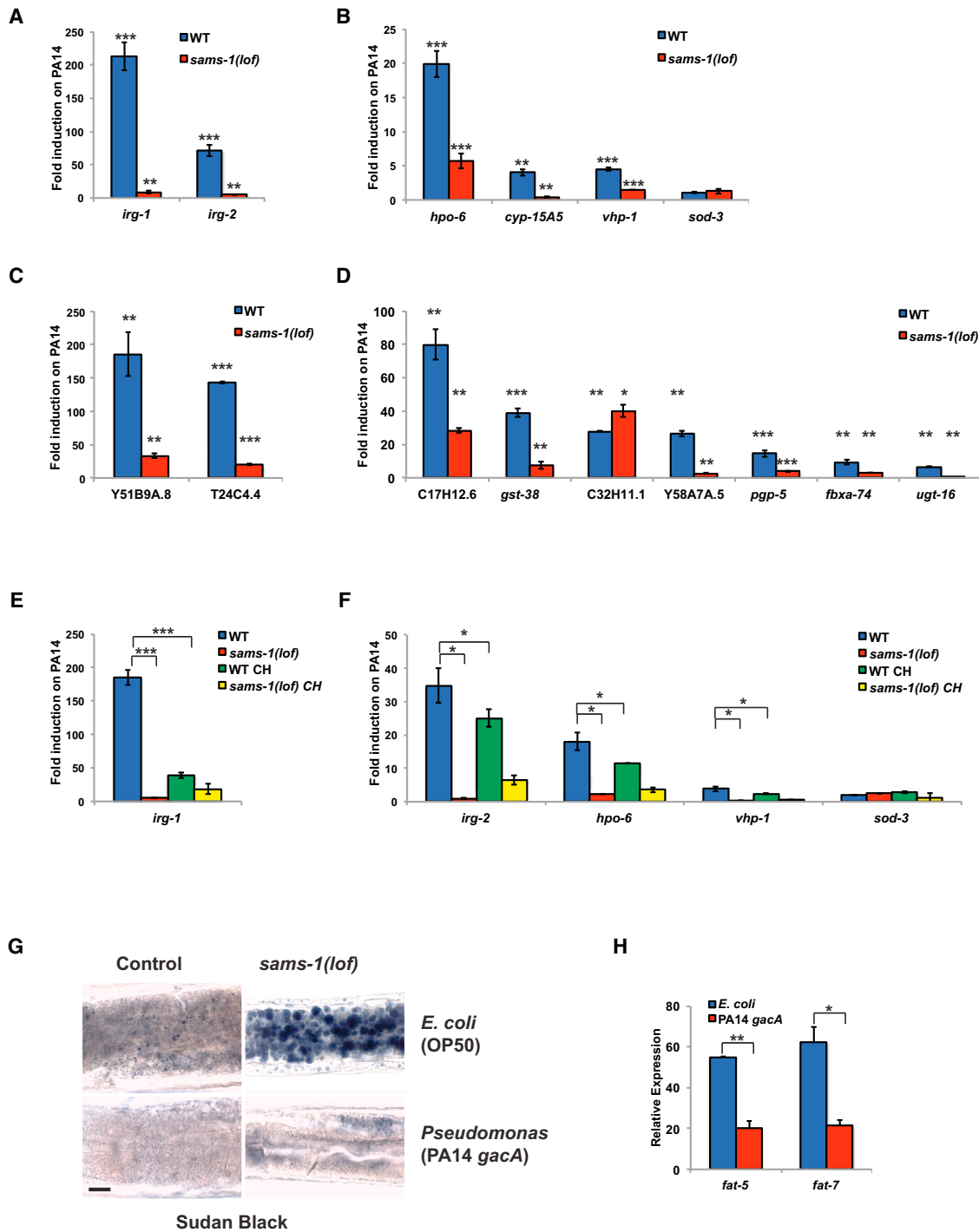
(E and F) Representative experiments showing quantitation of PA14 GFP and OP50 GFP after 24 (E) or 48 (F) hours exposure. Number of animals is shown in parentheses. “Partial” refers to light GFP in a section of the intestine, “full light” to light GFP along the length of the intestine and “full bright” to strong GFP in the entire intestinal tract.

criteria. First, we examined dynamics of *Pseudomonas*-induced gene expression when *C. elegans* were raised on choline as SAM-independent source of PC. We found that choline supplementation did not rescue the failure of infection response gene induction on *Pseudomonas* in *sams-1(lof)* animals (Figures 5E and 5F). Second, *Pseudomonas*, unlike *E. coli*, synthesizes PC (Malek et al., 2012). This PC appears sufficient to rescue lipid droplet formation and lipogenic gene expression in *sams-1* animals exposed to attenuated *Pseudomonas* strains for 48 hr (Figures 5G and 5H), suggesting that *C. elegans* fed *Pseudomonas* are not PC restricted. Thus, defects in infection response gene

induction seem unlikely to be linked to PC production and rather is likely to depend on other SAM-dependent methyltransferases.

Alterations in H3K4 Methylation in *sams-1* Animals

Although most gene expression changes in *sams-1(RNAi)* animals in basal conditions on *E. coli* are linked to changes in PC (Figure 3A), we reasoned that rapid transcriptional remodeling after contact with *Pseudomonas* might reveal requirements for SAM in histone methylation, as modifications are reconfigured along with gene expression. We focused on activating methylation marks such as H3K4me3 that are associated with

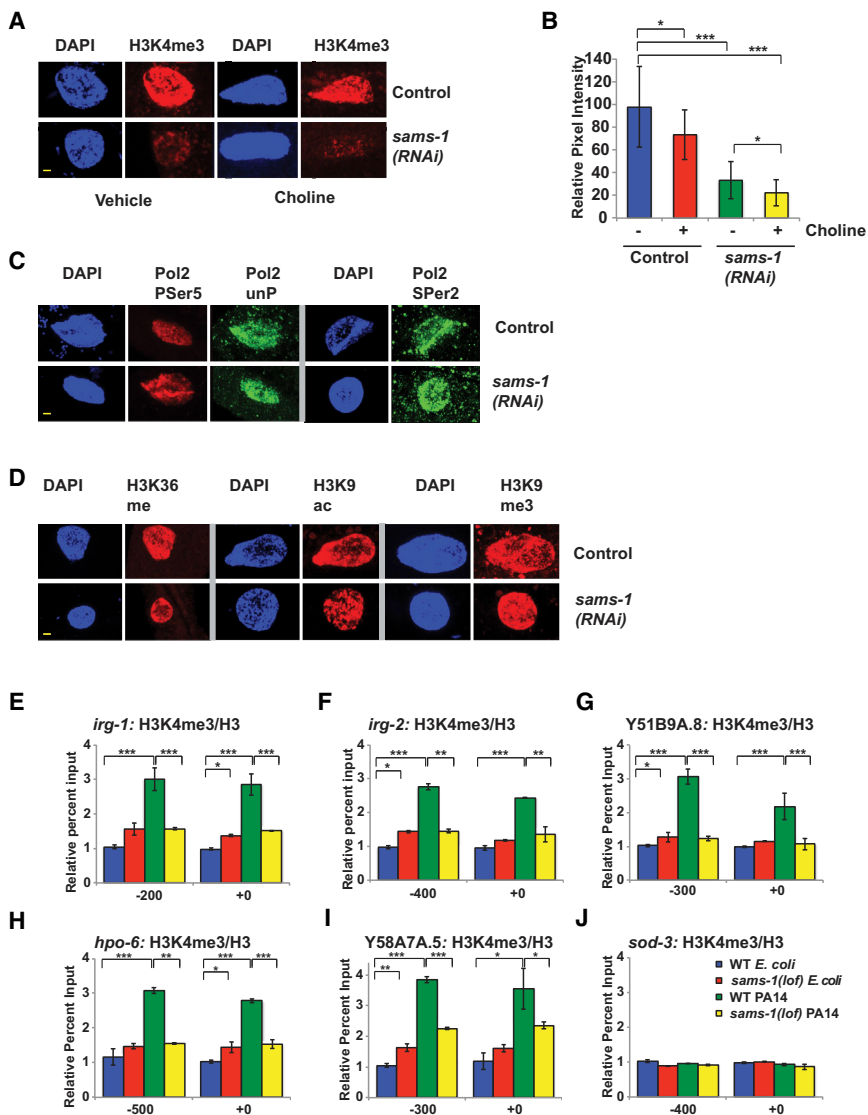
**Figure 5. *sams-1(lof)* Animals Lack a Transcriptional Response to Pathogens**

qRT-PCR comparing induction of infection response genes by *Pseudomonas* in wild-type (WT) or *sams-1(lof)* mutants after 6 hr of exposure to PA14 compared to the value on *E. coli* (OP50).

(A–D) Infection response genes were selected from innate immune genes with moderate induction on *E. coli* (OP50) after *sams-1(RNAi)* (A and B) or were selected from Troemel et al. (2006) (C and D).

(E and F) Induction of infection response genes in *sams-1(lof)* and *sams-1(lof)* choline (CH) rescued animals were compared by qRT-PCR.

(G and H) Lipid droplet accumulation shown by Sudan Black staining in anterior intestine (G) and lipogenic gene expression shown by qRT-PCR (H) comparing *C. elegans* maintained on *E. coli* and those raised on *E. coli* and transferred at L4 to *Pseudomonas gacA* for 48 hr. Error bars show SD. Results from Student's t test shown by * <0.05 , ** <0.01 , *** <0.005 .



high-level gene expression in a variety of species, including *C. elegans* (Shilatifard, 2012). H3K4me3 has been shown to vary as SAM levels change in cultured cells (Shyh-Chang et al., 2013), as well as in mouse liver (Kraus et al., 2014). To determine if H3K4 methylation was an important determinant in pathogen-induced gene expression, we examined several parameters. First, we used immunostaining to compare levels of H3K4me3 in wild-type and *sams-1(RNAi)* animals and found broad decreases in the global H3K4me3 levels in intestinal cells (Figures 6A and 6B; Figure S2A). Specificity of H3K4me3 can be seen by staining on autosomes, but not transcriptionally inactive X chromosome in pachytene nuclei (Bean et al., 2004) (Figure S2B). This decrease was unaffected by dietary choline (Figures 6A and 6B; Figure S2A), providing further evidence that decreases in H3K4 methylation are independent of PC-based pathways and could be directly affected by SAM levels.

Although changes in H3K4 methylation are not predicted to affect transcription globally in basal conditions (Weiner et al., 2012), we confirmed that reduction in SAM does not have global

Figure 6. Infection Response Genes Do Not Accumulate Activating Histone Methylation Marks in *sams-1(lof)* Mutants Exposed to *Pseudomonas*

(A) H3K4me3 is diminished in nuclei of intestinal cells after *sams-1(RNAi)* and in choline-treated *sams-1(RNAi)*. Yellow bar shows 2 μm.

(B) Quantitation of immuno fluorescence showing an average of pixel intensity over area for 8–12 nuclei per sample.

(C) Immunostaining comparing markers of active phosphorylated RNA Polymerase II (Pol II PSer 5, PSer 2) with total Pol II (unP). See Figure S2 for quantitation.

(D) Other histone modifications associated with active transcription (H3K36me and H3K9ac) or with heterochromatin (H3K9me3) within intestinal nuclei in control or *sams-1(RNAi)* animals. See Figure S2 for quantitation.

(E–J) Chromatin immunoprecipitation comparing levels of H3K4me3 on infection response or control genes grown on *E. coli* (OP50) or *Pseudomonas* (PA14) in wild-type (WT) or *sams-1(lof)* mutants. Input levels were normalized to the WT *E. coli* value on the upstream primer pair. Numerical representation of primer location is based on translational start site. Legend in (J) refers to all images. Error bars show SD. Results from Student's t test shown by * <0.05 , ** <0.01 , *** <0.005 .

effects on transcription by examining nuclear levels of transcribing RNA Pol II (Figure 6C; Figures S2C–S2F). Neither promoter-associated Pol II phosphorylated on Ser5 of the C-terminal domain (CTD) or Pol II CTD phospho-Ser2 (enriched in open reading frames) (Hsin and Manley, 2012) differed significantly between *sams-1(RNAi)* and controls. Furthermore, nuclear levels of H3K36 methylation, which like Pol II Ser2, maps to open reading frames of actively trans-

cribed genes (Shilatifard, 2006), or H3K9 acetylation, which is specific to promoter regions (Shilatifard, 2006) appeared equivalent in control and *sams-1(RNAi)* animals (Figure 6D; Figures S2G and S2H). We also found no changes in a repressive methylation mark, H3K9me3 (Figure 6D; Figure S2I). Thus, it appears that most basal transcriptional functions in *E. coli*-fed *sams-1(RNAi)* intestinal nuclei occur normally despite decreases in SAM levels and nuclear staining with antibodies to H3K4me3.

We next sought to determine if the dynamic responses of infection response genes upon *Pseudomonas* exposure were accompanied by changes in H3K4me3. Using chromatin immunoprecipitations with antibodies specific to H3K4me3 (see Figure S2I: *pcaf-1* 5' and 3', (Xiao et al., 2011)), we found that wild-type animals increased H3K4me3 levels at infection response genes upon exposure to virulent *Pseudomonas* (Figures 6E–6I), consistent with robust transcriptional activation of these genes (Figures 5A–5D). Importantly, increases in H3K4me3 did not occur in *sams-1(lof)* animals exposed to

Pseudomonas, correlating strongly with the failure to induce these genes.

We also examined H3K4me3 levels on control genes with similar expression levels on *E. coli* and *Pseudomonas*. The oxidative stress response gene *sod-3*, the control gene *pcaf-1*, and non-intestinally expressed gene *odr-10* showed equivalent H3K4me3 methylation in both control and PA14 samples (Figure 6J; Figures S2J and S2K), showing that H3K4me3 hypermethylation upon *Pseudomonas* exposure was linked to dynamic increases in expression of those genes. In apparent contrast to significant decreases in global H3K4me3 seen in immunofluorescence of *sams-1(RNAi)* intestinal nuclei, H3K4me3 was not decreased in basal conditions on infection response genes, *pcaf-1*, *sod-3* or *odr-10*. Therefore we compared H3K4me3 levels at the start site for genes expressed at high levels in the intestine as well as other tissues (*ama-1*, *rpb-2*, *act-1*, *arf-1.1* and *taf-1*), an intestinal specific gene (*ges-1*) and a gene not expressed in hermaphrodites (*her-1*) with control intragenic primers (Figure S2I). We found that H3K4me3 was significantly enriched at the control gene start sites in both wild-type and *sams-1(lf)* for the intestinally expressed genes, suggesting that the broad decrease in global H3K4me3 could reflect other genes or differences in sensitivity between immunofluorescence and chromatin immunoprecipitation. Taken together, our assays suggest that deficits in SAM have the greatest effects on promoters with dynamic changes expression and in H3K4me3.

set-16/MLL Is Critical for Transcriptional Response to Pathogenic Stress

H3K4 modification may occur through the action of several methyltransferases that function in the COMPASS methyltransferase complex (Shilatifard, 2012). *C. elegans* contains orthologs of catalytic COMPASS complex components such as *set-2/SETD1A*/*KMT2F/Set1* and *set-16/MLL/KMT2A* (Wenzel et al., 2011), which function in germline-dependent transgenerational regulation of lifespan and also in development (Greer et al., 2010, 2011; Li and Kelly, 2011; Xiao et al., 2011). We next asked which H3K4 methyltransferases were most important for global histone methylation in the intestine and for induction of infection response genes. *set-2/SET1* is reported to function as the major H3K4 methyltransferase in the distal germline as well as during development (Li and Kelly, 2011; Xiao et al., 2011). Consistent with these observations, H3K4me3 is significantly reduced in *set-2(RNAi)* intestinal nuclei (Figures 7A and 7B), although the characteristic autosome-specific staining pattern can be seen in pachytene nuclei (Figure S3A). Strikingly, infection response gene induction after *set-2/SET1(RNAi)* occurs normally, suggesting *set-2/SET1* does not play an essential role in the transcriptional response to *Pseudomonas* (Figures 7C–7E). In contrast, *set-16/MLL* knockdown showed a more moderate decreases in global nuclear levels of H3K4me3 in intestinal nuclei (Figures 7A and 7B), but was necessary for complete induction of the majority of infection response genes (Figures 7F–7H). As with *sams-1*, we found that *set-16* was necessary for H3K4me3 at infection response gene promoters (Figures S3B–S3E) and that histone methylation was similar between control and *set-16(RNAi)* samples on control genes (Figure S3F). Consistent with this observation, candidate lists from an RNAi screen for genes important for *irg-1::GFP* induction on *Pseudomonas*

include T12D8.1 (identified as *set-16*) (Estes et al., 2010). This suggests genes requiring *set-16/MLL*-dependent methylation may be preferentially affected by SAM depletion during the transcriptional response to pathogens.

DISCUSSION

The 1-carbon cycle links dietary levels of folate and B₁₂ to nucleotide production, protection from oxidative stress, and synthesis of the methyl donor SAM (Lu and Mato, 2008). Diverse cellular pathways are affected by methylation, including epigenetic modification of histones or DNA (Kaelin and McKnight, 2013), phospholipid production (Vance, 2014), RNA modification (Ha and Kim, 2014), and the reach of non-histone protein methylation is only partly described (Moore et al., 2013). Many studies addressing physiological roles of methylation have focused on inactivating specific methyltransferases complexes; however, reductions in SAM due to dietary deficiencies, genetic polymorphisms or environmental factors may not impact all methyltransferases equivalently, therefore it has been difficult to discern how changes in SAM levels interface with molecular mechanisms.

We have made important new connections between SAM levels and phenotypes associated with metabolic disease by determining which methylation-dependent pathways are most sensitive to SAM depletion on different diets and stress conditions. In *C. elegans* living on *E. coli*, *sams-1(RNAi)* or loss of function results in accumulation of lipid droplets (Walker et al., 2011), lifespan extension (Hansen et al., 2005), and upregulation of innate immune signatures. The upregulation of lipogenesis or PMK-1-dependent innate immunity appears linked to decreased PC because both phenotypes are rescued by dietary choline. However, lipogenesis and innate immune activation appear regulated by distinct mechanisms downstream of PC, since innate immune genes do not appear to be activated by the SBP-1/SREBP-1 transcription factors driving lipogenesis. PC is both an integral membrane component and a substrate for phospholipases involved in signaling (Vance 2014). Low PC could non-specifically alter basic membrane properties and induce PMK-1 similarly to mechanisms sensing epidermal wounding (Zugasti et al., 2014) or the action of pore forming toxin (Huffman et al., 2004). However, as in the case of low cholesterol activation of SREBP in mammals (Osborne and Espenshade, 2009), levels of membrane lipids may also act as part of highly specific molecular mechanisms to change protein activity. Stimulation of innate immunity has been suggested as the “second hit” in the development of fatty liver disease after lipid accumulation (Jin et al., 2013), therefore, finding that both lipogenic and specific innate immune gene expression programs can be affected by changes in SAM/PC levels is striking and suggests that these distinct phenotypes could be regulated by similar metabolic dysfunctions.

Exposure of *sams-1* animals to *Pseudomonas*, on the other hand, elicits a distinct set of metabolic and stress-related phenotypes. In surprising contrast to innate immune activation and lifespan extension when fed *E. coli*, *sams-1(lf)* animals die rapidly when exposed to virulent *Pseudomonas* and do not implement critical transcriptional responses to bacterial stress. Despite global decreases in H3K4me3, we do not find evidence

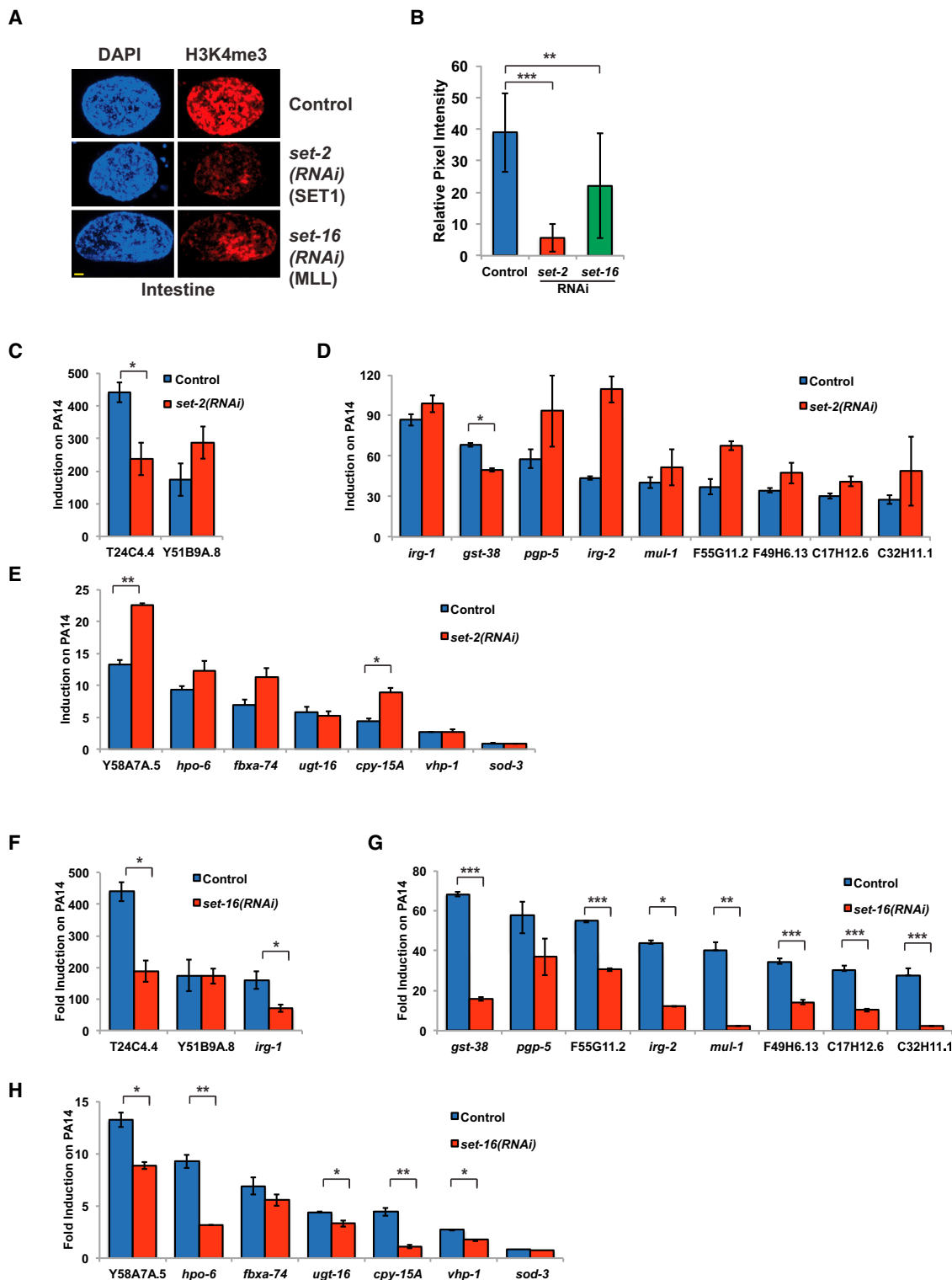


Figure 7. set-16/MLL Is Important for Expression of Infection Response Genes upon *Pseudomonas* Exposure

(A) Immunostaining of intestinal nuclei with antibodies to H3K4me3 after RNAi of set-2 or set-16. Yellow bar shows 2 μ m.
(B) Quantitation of immunofluorescence showing an average of pixel intensity over area for 8–12 nuclei per sample. Requirement for set-2/SET1 (B–D) or set-16/MLL (E–H) for induction of infection response genes upon a 6 hr exposure to PA14 compared to *E. coli* (HT115). Error bars show SD. Results from Student's t test shown by * <0.05 , ** <0.01 , *** <0.005 .

that basal transcriptional processes are altered. Rather, the biological effects of decreased SAM emerge when new transcription to combat *Pseudomonas* becomes essential. H3K4me3 accumulation accompanies infection response gene induction in wild-type animals, but is absent in *sams-1(lop)* animals, suggesting transcriptional consequences of H3K4me3 deficiency are evident under conditions that promote large-scale changes in gene expression.

It is also striking that the H3K4 methyltransferase *set-16/MLL*, which has a less dramatic effect on total methylation than *set-2/SET1*, has a more critical role inducing infection response genes in response to *Pseudomonas*. Interestingly, MLL has been proposed to bookmark genes that have the highest dynamic range of gene expression as cells exit mitosis, while SET1 may be important for maintaining H3K4 methylation (Blobel et al., 2009). Several studies have shown global H3K4 methylation likely to be affected when SAM is limiting (Kraus et al., 2014; Shyh-Chang et al., 2013), however, we find that SAM depletion specifically mirrors *set-16/MLL*-dependent effects on stress-induced gene expression.

Extensive studies have highlighted the importance of chromatin-regulatory complexes affecting histone methylation (Shi latifard, 2012; Weiner et al., 2012), or the need SAM to support PC synthesis in the liver (Vance, 2014). However, mechanistic links between SAM levels and phenotypes associated with metabolic disease have been difficult to discern. Our studies in the *C. elegans* pathogen response suggest that *sams-1* can preferentially affect *set-16*-dependent H3K4 methylation. Interestingly, Twobin et al. have found that a different SAM synthase, *sams-3*, is important for repressive H3K9 methylation (Towbin et al., 2012), suggesting methyltransferases might access distinct pools of SAM or require interactions with specific synthases. Several important studies have focused on effects of altering histone methylation in *C. elegans* through inactivating H3K4 methylation complexes and found transgenerational germline-dependent consequences on lifespan (Greer et al., 2010; Greer et al., 2011). Our studies demonstrate that SAM depletion significantly affects physiology by limiting acute transcriptional responses to stress. Finally, because depletion of SAM affects multiple methylation-dependent pathways, understanding physiological impacts of methyl donor limitation requires integration of phospholipid- and chromatin-mediated effects on cellular function.

EXPERIMENTAL PROCEDURES

C. elegans Strains and RNAi Constructs

N2 (wild-type), *pmk-1(ku25)*, *tir-1(tm3036)*, OP50, and OP50 GFP were obtained from the Caenorhabditis Genetics Center; PA14, PA14 *gacA*, and PA14 GFP were gifts from the Ausubel lab. Normal growth media (NGM) was used unless otherwise noted; choline was added to 30 mM where described. HA1975 *sams-1(ok3033)* is described in Walker et al. (2011). Control RNAi is L4440; X-5P21 was used for *sams-1(RNAi)*; *set-2* and *set-16* RNAi were performed with Orfome clone C26E6.9 (Rual et al., 2004) and III-6D12 from the Ahringer RNAi library (Simmer et al., 2003), respectively.

Gene Expression Analysis

L4/young adult *C. elegans* were lysed in 0.5% SDS, 5% β-ME, 10 mM EDTA, 10 mM Tris-HCl pH 7.4, 0.5 mg/ml Proteinase K, then RNA was purified with Tri-Reagent (Sigma). RNA for microarrays was purified by RNAeasy columns (QIAGEN). For control, *sams-1*, and *sbp-1(RNAi)* comparisons (Figures 1B

and 1G), Affymetrix Gene 1.1 *C. elegans* exon tiling arrays were used. Affymetrix *C. elegans* arrays (GeneChip *C. elegans* Genome Arrays) were used for comparison of control, *sams-1(RNAi)*, control choline, and *sams-1(RNAi)* choline samples (Figures 3A–3C). cDNA synthesis and array hybridization were carried out by the UMASS Microarray core facility. For whole-genome analysis, significant genes were defined as changing >2.0-fold with p < 0.05. GOrilla (RRID: nlx_80425; <http://cbl-gorilla.cs.technion.ac.il>) (Eden et al., 2009) and REViGO (RRID: nlx_149332; <http://revigo.irb.hr>) were used for GO term analysis. cDNA for quantitative RT-PCR was prepared with the Invitrogen Transcripter kit. cDNA was standardized to *act-1*, except for Figures 1C–1F where a “spike in” control was used. Briefly, 20 pg of in vitro translated (Ambion Megascript) human JNK1alpha1 RNA was added to *C. elegans* samples before cDNA synthesis and PCR was quantitated against this absolute standard. Primers for qPCR are available upon request. Representative experiments from at least three repetitions are shown.

Immunoblotting

C. elegans at the L4/young adult transition were sonicated in RIPA (50 mM Tris, pH 8.0, 150 mM sodium chloride, 1% NP40, 0.1% sodium dodecyl sulfate, 0.5% sodium deoxycholate) containing 1 mM DTT, Complete Protease Inhibitors (Roche), Phosphostop (Roche), and ALLN (Calbiochem). Equal amounts of protein were separated, transferred to nitrocellulose, and probed with antibodies to phospho p38 (Cell Signaling, RRID: AB_331640), *sams-1* (MAT1A 4D11, Novus Biologicals, RRID: AB_1214674), and Histone 3 (Cell Signaling, RRID: AB_532248). Immune complexes were depicted with ImmobilonTM Luminol Reagent (Millipore).

Lipid Analysis

For lipid analysis by thin-layer chromatography and gas chromatography-mass spectrometry, mid-L4 larvae were harvested and snap-frozen in liquid N₂, stored at –80°C before lipids extracted, separated, and quantified as described (Hou et al., 2014).

Pseudomonas Treatment

Pseudomonas strains were grown 15 hr in liquid culture, spread to edges of slow kill agar in 60 mM tissue culture plates, and prepared as in (Powell and Ausubel, 2008). For sterilization, gravid hermaphrodites were placed on *cdc-25(RNAi)* for 6 hr before bleaching to *cde-25(RNAi)* plates (Shapira and Tan, 2008). More than 100 L4 larvae were added to replicate plates of PA14 or PA14 *gacA* and were incubated at 25 degrees. OASIS was used to generate Kaplan-Meier plots (Yang et al., 2011). In parallel with pathogenicity assays, more than 30 *C. elegans* young adults sterilized by *cde-25(RNAi)* were plated onto NGM/OP50 plates and incubated at 20°C. For analysis of PA14 GFP or OP50 GFP, animals were removed at 24 and 48 hr and imaged on a Leica TCS SPE II. For images of whole worms, composite images were pasted to gray (DIC) or black (GFP) backgrounds. For analysis of *Pseudomonas*-induced effects on gene expression, protein levels, or chromatin modification, *C. elegans* were grown on *E. coli* until L4/young adult, then re-plated on to *E. coli* or PA14 and incubated for 6 hr at 25°C.

Immunofluorescence

For H3K4me3 (RRID: AB_836882), dissected intestines were incubated in 2% paraformaldehyde, freeze cracked, then treated with –20°C ethanol before washing in PBS, 1% Tween-20, and 0.1% BSA (Li and Kelly, 2011). For H3K9me3 (RRID: AB_2115268), H3K9ac (RRID: AB_823528), or H3K36 (RRID: AB_2295073), –20°C methanol was used and washes or blocking were performed in PBS, 1% Triton X-100, and 0.1% BSA. For RNA Pol II Antibodies (PSer2, Abcam, RRID: AB_2167352; PSer5, Abcam, RRID: AB_5095; UnP, Abcam, RRID: AB_306327), slides were freeze cracked, fixed in ×20°C methanol, then 3.7% formaldehyde, and incubated in PBS/Triton blocking solution (Walker et al., 2007). Images were taken on a Leica SPE II at identical gain settings within experimental sets. Quantitation was derived for pixel intensity over nuclear area for at least ten nuclei. Levels corrections in Adobe Photoshop were performed uniformly across experimental sets.

Sudan Black Staining

Second-day adult *C. elegans* were fixed in 1% paraformaldehyde before three freeze thaw cycles. Samples were washed in 25%, 50%, and 75% ethanol

before staining overnight in a 1:1 dilution of Sudan Black in 75% ethanol. After rehydration, imaging was performed by brightfield microscopy on a Leica SPE II.

Chromatin Immunoprecipitation

L4/young adult *C. elegans* were collected and frozen at -80°C. Frozen pellets were ground and resuspended in 5 volumes of hypotonic lysis buffer (250 mM sucrose, 10 mM KCl, 1.5 mM MgCl₂, 1 mM EGTA, 1 mM DTT, plus complete protease inhibitors) and dounced with pestle A, then nuclei were separated by centrifugation. Crosslinking reactions, performed in 1% formaldehyde, were stopped by 100 mM glycine before sonication. Ten micrograms of lysate was pre-cleared with Protein A/G Dynabeads (Invitrogen), then incubated with antibodies to H3K4me3 (Cell Signaling) or Histone 3 (Cell Signaling, RRID: AB_1904005). Immune complexes were precipitated with Protein A/G (Invitrogen). For quantitative PCR, a standard curve for each primer pair was used to determine the amount of DNA/Ct value and percent of input was determined and used for comparison between samples.

SUPPLEMENTAL INFORMATION

Supplemental Information includes three figures and four tables and can be found with this article online at <http://dx.doi.org/10.1016/j.cmet.2015.07.013>.

AUTHOR CONTRIBUTIONS

Conceptualization: A.K.W.; Methodology: S.T., J.L.W., and A.K.W.; Formal Analysis: A.K.W.; Investigation: W.D., L.J.S., N.B., N.S.H., J.L.W., S.T., and A.K.W.; Resources: W.D. and N.S.H.; Writing – Original Draft: A.K.W.; Writing – Review & Editing: W.D., L.J.S., J.L.W., S.T., and A.K.W.; Funding Acquisition: J.L.W., S.T., and A.K.W.

ACKNOWLEDGMENTS

We would like to acknowledge Dr. Yvonne Edwards for bioinformatics and Xun Shi for technical assistance with lipid analysis. We are grateful to Drs. Tom Fazzio, Oliver Rando (UMASS) and Francesca Palladino (Ecole Normale Supérieure de Lyon, Lyon, France) for advice on chromatin immunoprecipitation protocols. We also thank Dr. Jonathan Ewbank for discussing our microarray data and to the lab of Dr. Frederick Ausubel for *Pseudomonas* strains. We thank Dr. Marian Walhout for invaluable comments on the manuscript, as well as Drs. Thomas Fazzio and Dr. Brendan Kiernan for critical reading. Some *C. elegans* strains were provided by the Caenorhabditis Genetics Center (CGC), funded by NIH Office of Research Infrastructure Programs (P40 OD010440). N.S.H. was supported by scholarships from the University of British Columbia (UBC) and the Child and Family Research Institute (CFRI). This work was supported by the NIH through R01DK084352 (to A.K.W.) and R01DK74114 (to J.W.), and by CIHR MOP-93713, NSERC RGPIN 386398-13, and a Canada Research Chair (to S.T.).

Received: March 2, 2015

Revised: May 29, 2015

Accepted: July 17, 2015

Published: August 27, 2015

REFERENCES

- Bean, C.J., Schaner, C.E., and Kelly, W.G. (2004). Meiotic pairing and imprinted X chromatin assembly in *Caenorhabditis elegans*. *Nat. Genet.* 36, 100–105.
- Blobel, G.A., Kadouke, S., Wang, E., Lau, A.W., Zuber, J., Chou, M.M., and Vakoc, C.R. (2009). A reconfigured pattern of MLL occupancy within mitotic chromatin promotes rapid transcriptional reactivation following mitotic exit. *Mol. Cell* 36, 970–983.
- Couillaud, C., Pujol, N., Reboul, J., Sabatier, L., Guichou, J.-F., Kohara, Y., and Ewbank, J.J. (2004). TLR-independent control of innate immunity in *Caenorhabditis elegans* by the TIR domain adaptor protein TIR-1, an ortholog of human SARM. *Nat. Immunol.* 5, 488–494.
- Eden, E., Navon, R., Steinfeld, I., Lipson, D., and Yakhini, Z. (2009). GOrilla: a tool for discovery and visualization of enriched GO terms in ranked gene lists. *BMC Bioinformatics* 10, 48.
- Engelmann, I., Griffon, A., Tichit, L., Montañana-Sanchis, F., Wang, G., Reinke, V., Waterston, R.H., Hillier, L.W., and Ewbank, J.J. (2011). A comprehensive analysis of gene expression changes provoked by bacterial and fungal infection in *C. elegans*. *PLoS ONE* 6, e19055.
- Estes, K.A., Dunbar, T.L., Powell, J.R., Ausubel, F.M., and Troemel, E.R. (2010). bZIP transcription factor zip-2 mediates an early response to *Pseudomonas aeruginosa* infection in *Caenorhabditis elegans*. *Proc. Natl. Acad. Sci. USA* 107, 2153–2158.
- Greer, E.L., Maures, T.J., Hauswirth, A.G., Green, E.M., Leeman, D.S., Maro, G.S., Han, S., Banko, M.R., Gozani, O., and Brunet, A. (2010). Members of the H3K4 trimethylation complex regulate lifespan in a germline-dependent manner in *C. elegans*. *Nature* 466, 383–387.
- Greer, E.L., Maures, T.J., Ucar, D., Hauswirth, A.G., Mancini, E., Lim, J.P., Benayoun, B.A., Shi, Y., and Brunet, A. (2011). Transgenerational epigenetic inheritance of longevity in *Caenorhabditis elegans*. *Nature* 479, 365–371.
- Ha, M., and Kim, V.N. (2014). Regulation of microRNA biogenesis. *Nat. Rev. Mol. Cell Biol.* 15, 509–524.
- Halsted, C.H., Villanueva, J.A., Devlin, A.M., Niemelä, O., Parkkila, S., Garrow, T.A., Wallock, L.M., Shigenaga, M.K., Melnyk, S., and James, S.J. (2002). Folate deficiency disturbs hepatic methionine metabolism and promotes liver injury in the ethanol-fed micropig. *Proc. Natl. Acad. Sci. USA* 99, 10072–10077.
- Hansen, M., Hsu, A.L., Dillin, A., and Kenyon, C. (2005). New genes tied to endocrine, metabolic, and dietary regulation of lifespan from a *Caenorhabditis elegans* genomic RNAi screen. *PLoS Genet.* 1, 119–128.
- Hou, N.S., Gutschmidt, A., Choi, D.Y., Pather, K., Shi, X., Watts, J.L., Hoppe, T., and Taubert, S. (2014). Activation of the endoplasmic reticulum unfolded protein response by lipid disequilibrium without disturbed proteostasis *in vivo*. *Proc. Natl. Acad. Sci. USA* 111, E2271–E2280.
- Hsin, J.P., and Manley, J.L. (2012). The RNA polymerase II CTD coordinates transcription and RNA processing. *Genes Dev.* 26, 2119–2137.
- Huffman, D.L., Abrami, L., Sasik, R., Corbeil, J., van der Goot, F.G., and Aroian, R.V. (2004). Mitogen-activated protein kinase pathways defend against bacterial pore-forming toxins. *Proc. Natl. Acad. Sci. USA* 101, 10995–11000.
- Im, S.S., Yousef, L., Blaschitz, C., Liu, J.Z., Edwards, R.A., Young, S.G., Raffatellu, M., and Osborne, T.F. (2011). Linking lipid metabolism to the innate immune response in macrophages through sterol regulatory element binding protein-1a. *Cell Metab.* 13, 540–549.
- Irazoqui, J.E., Troemel, E.R., Feinbaum, R.L., Luhachack, L.G., Cezairliyan, B.O., and Ausubel, F.M. (2010). Distinct pathogenesis and host responses during infection of *C. elegans* by *P. aeruginosa* and *S. aureus*. *PLoS Pathog.* 6, e1000982.
- Jin, C., Henao-Mejia, J., and Flavell, R.A. (2013). Innate immune receptors: key regulators of metabolic disease progression. *Cell Metab.* 17, 873–882.
- Kaelin, W.G., Jr., and McKnight, S.L. (2013). Influence of metabolism on epigenetics and disease. *Cell* 153, 56–69.
- Kawli, T., and Tan, M.W. (2008). Neuroendocrine signals modulate the innate immunity of *Caenorhabditis elegans* through insulin signaling. *Nat. Immunol.* 9, 1415–1424.
- Kim, D.H. (2013). Bacteria and the aging and longevity of *Caenorhabditis elegans*. *Annu. Rev. Genet.* 47, 233–246.
- Kim, D.H., Feinbaum, R., Alloing, G., Emerson, F.E., Garsin, D.A., Inoue, H., Tanaka-Hino, M., Hisamoto, N., Matsumoto, K., Tan, M.W., and Ausubel, F.M. (2002). A conserved p38 MAP kinase pathway in *Caenorhabditis elegans* innate immunity. *Science* 297, 623–626.
- Kraus, D., Yang, Q., Kong, D., Banks, A.S., Zhang, L., Rodgers, J.T., Pirinen, E., Pulinkunnel, T.C., Gong, F., Wang, Y.C., et al. (2014). Nicotinamide N-methyltransferase knockdown protects against diet-induced obesity. *Nature* 508, 258–262.
- Kurz, C.L., and Tan, M.W. (2004). Regulation of aging and innate immunity in *C. elegans*. *Aging Cell* 3, 185–193.

- Li, T., and Kelly, W.G. (2011). A role for Set1/MLL-related components in epigenetic regulation of the *Caenorhabditis elegans* germ line. *PLoS Genet.* 7, e1001349.
- Lu, S.C., and Mato, J.M. (2008). S-Adenosylmethionine in cell growth, apoptosis and liver cancer. *J. Gastroenterol. Hepatol.* 23 (Suppl 1), S73–S77.
- Lu, S.C., Alvarez, L., Huang, Z.Z., Chen, L., An, W., Corrales, F.J., Avila, M.A., Kanel, G., and Mato, J.M. (2001). Methionine adenosyltransferase 1A knockout mice are predisposed to liver injury and exhibit increased expression of genes involved in proliferation. *Proc. Natl. Acad. Sci. USA* 98, 5560–5565.
- MacNeil, L.T., Watson, E., Arda, H.E., Zhu, L.J., and Walhout, A.J.M. (2013). Diet-induced developmental acceleration independent of TOR and insulin in *C. elegans*. *Cell* 153, 240–252.
- Malek, A.A., Wargo, M.J., and Hogan, D.A. (2012). Absence of membrane phosphatidylcholine does not affect virulence and stress tolerance phenotypes in the opportunistic pathogen *Pseudomonas aeruginosa*. *PLoS ONE* 7, e30829.
- Mato, J.M., Martínez-Chantar, M.L., and Lu, S.C. (2008). Methionine metabolism and liver disease. *Annu. Rev. Nutr.* 28, 273–293.
- Moore, K.E., Carlson, S.M., Camp, N.D., Cheung, P., James, R.G., Chua, K.F., Wolf-Yadlin, A., and Gozani, O. (2013). A general molecular affinity strategy for global detection and proteomic analysis of lysine methylation. *Mol. Cell* 50, 444–456.
- Osborne, T.F., and Espenshade, P.J. (2009). Evolutionary conservation and adaptation in the mechanism that regulates SREBP action: what a long, strange tRIP it's been. *Genes Dev.* 23, 2578–2591.
- Petrosian, T.C., and Clarke, S.G. (2011). Uncovering the human methyltransferasome. *Mol. Cell. Proteomics* 10, M110 000976.
- Powell, J.R., and Ausubel, F.M. (2008). Models of *Caenorhabditis elegans* infection by bacterial and fungal pathogens. *Methods Mol. Biol.* 415, 403–427.
- Rual, J.F., Ceron, J., Koreth, J., Hao, T., Nicot, A.S., Hirozane-Kishikawa, T., Vandenhoute, J., Orkin, S.H., Hill, D.E., van den Heuvel, S., and Vidal, M. (2004). Toward improving *Caenorhabditis elegans* genome mapping with an ORFeome-based RNAi library. *Genome Res.* 14 (10B), 2162–2168.
- Shapira, M., and Tan, M.-W. (2008). Genetic analysis of *Caenorhabditis elegans* innate immunity. *Methods Mol. Biol.* 415, 429–442.
- Shilatifard, A. (2006). Chromatin modifications by methylation and ubiquitination: implications in the regulation of gene expression. *Annu. Rev. Biochem.* 75, 243–269.
- Shilatifard, A. (2012). The COMPASS family of histone H3K4 methylases: mechanisms of regulation in development and disease pathogenesis. *Annu. Rev. Biochem.* 81, 65–95.
- Shyh-Chang, N., Locasale, J.W., Lyssiotis, C.A., Zheng, Y., Teo, R.Y., Ratanasirinawoot, S., Zhang, J., Onder, T., Unternaehrer, J.J., Zhu, H., et al. (2013). Influence of threonine metabolism on S-adenosylmethionine and histone methylation. *Science* 339, 222–226.
- Simmer, F., Moorman, C., van der Linden, A.M., Kuijk, E., van den Berghe, P.V., Kamath, R.S., Fraser, A.G., Ahringer, J., and Plasterk, R.H. (2003). Genome-wide RNAi of *C. elegans* using the hypersensitive *rrf-3* strain reveals novel gene functions. *PLoS Biol.* 1, E12.
- Tan, M.W., Rahme, L.G., Sternberg, J.A., Tompkins, R.G., and Ausubel, F.M. (1999). *Pseudomonas aeruginosa* killing of *Caenorhabditis elegans* used to identify *P. aeruginosa* virulence factors. *Proc. Natl. Acad. Sci. USA* 96, 2408–2413.
- Towbin, B.D., González-Aguilera, C., Sack, R., Gaidatzis, D., Kalck, V., Meister, P., Askjaer, P., and Gasser, S.M. (2012). Step-wise methylation of histone H3K9 positions heterochromatin at the nuclear periphery. *Cell* 150, 934–947.
- Troemel, E.R., Chu, S.W., Reinke, V., Lee, S.S., Ausubel, F.M., and Kim, D.H. (2006). p38 MAPK regulates expression of immune response genes and contributes to longevity in *C. elegans*. *PLoS Genet.* 2, e183.
- Vance, D.E. (2014). Phospholipid methylation in mammals: from biochemistry to physiological function. *Biochim. Biophys. Acta* 1838, 1477–1487.
- Walker, A.K., Boag, P.R., and Blackwell, T.K. (2007). Transcription reactivation steps stimulated by oocyte maturation in *C. elegans*. *Dev. Biol.* 304, 382–393.
- Walker, A.K., Jacobs, R.L., Watts, J.L., Rottiers, V., Jiang, K., Finnegan, D.M., Shiota, T., Hansen, M., Yang, F., Niebergall, L.J., et al. (2011). A conserved SREBP-1/phosphatidylcholine feedback circuit regulates lipogenesis in metazoans. *Cell* 147, 840–852.
- Wasmuth, J., Schmid, R., Hedley, A., and Blaxter, M. (2008). On the extent and origins of genic novelty in the phylum Nematoda. *PLoS Negl. Trop. Dis.* 2, e258.
- Watson, E., MacNeil, L.T., Arda, H.E., Zhu, L.J., and Walhout, A.J.M. (2013). Integration of metabolic and gene regulatory networks modulates the *C. elegans* dietary response. *Cell* 153, 253–266.
- Watson, E., MacNeil, L.T., Ritter, A.D., Yilmaz, L.S., Rosebrock, A.P., Caudy, A.A., and Walhout, A.J.M. (2014). Interspecies systems biology uncovers metabolites affecting *C. elegans* gene expression and life history traits. *Cell* 156, 759–770.
- Weiner, A., Chen, H.V., Liu, C.L., Rahat, A., Klien, A., Soares, L., Gudipati, M., Pfeffner, J., Regev, A., Buratowski, S., et al. (2012). Systematic dissection of roles for chromatin regulators in a yeast stress response. *PLoS Biol.* 10, e1001369.
- Wenzel, D., Palladino, F., and Jedrusik-Bode, M. (2011). Epigenetics in *C. elegans*: facts and challenges. *Genesis* 49, 647–661.
- Xiao, Y., Bedet, C., Robert, V.J.P., Simonet, T., Dunkelbarger, S., Rakotomalala, C., Soete, G., Korswagen, H.C., Strome, S., and Palladino, F. (2011). *Caenorhabditis elegans* chromatin-associated proteins SET-2 and ASH-2 are differentially required for histone H3 Lys 4 methylation in embryos and adult germ cells. *Proc. Natl. Acad. Sci. USA* 108, 8305–8310.
- Yang, J.S., Nam, H.J., Seo, M., Han, S.K., Choi, Y., Nam, H.G., Lee, S.J., and Kim, S. (2011). OASIS: online application for the survival analysis of lifespan assays performed in aging research. *PLoS ONE* 6, e23525.
- Zugasti, O., Bose, N., Squiban, B., Belougne, J., Kurz, C.L., Schroeder, F.C., Pujol, N., and Ewbank, J.J. (2014). Activation of a G protein-coupled receptor by its endogenous ligand triggers the innate immune response of *Caenorhabditis elegans*. *Nat. Immunol.* 15, 833–838.

Cell Metabolism

Supplemental Information

**s-Adenosylmethionine Levels Govern Innate Immunity
through Distinct Methylation-Dependent Pathways**

Wei Ding, Lorissa J. Smulan, Nicole S. Hou, Stefan Taubert, Jennifer L. Watts, and Amy K. Walker

Supplemental information

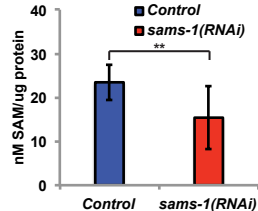
1. **Table S1.** List of genes and human orthologs. Refers to Figure 1.
2. **Table S2** (Microsoft Excel file). **Co-regulation of lipogenic and immune function genes with depletion of SAMe.** Refers to **Figure 1**
3. **Table S3** (Microsoft Excel files), **Choline rescues gene expression after *sams-1(RNAi)*.** Refers to **Figure 3**
4. **Figure S1.** **Choline rescues upregulation of lipogenic or innate immune genes in *sams-1(lof)* animals on *E. coli*.** Refers to **Figure 3**.
5. **Table S4** (Microsoft Excel file). Reduced resistance to *Pseudomonas aeruginosa* in *sams-1(lof)* animals. Statistical data for survival assays. Refers to **Figure 4**.
6. **Figure S2.** ***sams-1(lof)* mutants fail to accumulate activating histone methylation marks on infection response genes when exposed to *Pseudomonas*.** Refers to **Figure 6**.
7. **Figure S3.** ***set-16/MLL* is important for expression of infection response genes upon *Pseudomonas* exposure.** Refers to **Figure 7**.

<i>C. elegans</i>	Human	Description	Function	Class
<i>act-1</i>	ACTB	Beta actin	Cytoskeleton	Control gene
<i>ama-1</i>	RBP1	RNA Polymerase 2, large subunit	Basal transcription	Control gene
<i>arf-1.1</i>	ARF1	ADP-ribosylation factor 1	GTPase	Intracellular transport
C17H12.6			CUB-like domain	Infection response
C32H11.1			CUB domain protein	Infection response
<i>cyp-13A5</i>	CYP3A5	Cytochrome P450 3A5	monooxygenases	Infection response
<i>fat-7</i>	SCD	Steroyl CoA desaturase	Produces oleic acid	Fatty acid biosynthesis
<i>fbxa-74</i>		F-box protein	Ubiquitin ligase	Infection response
<i>ges-1</i>	CES1	gut esterase	Intestine function	Intestinal control gene
<i>gst-38</i>	HPGDS	Hematopoietic prostaglandin D synthase	Glutathione-S transferase	Infection response
<i>her-1</i>		Male specific secreted protein	Secreted protein	Male specific control gene
<i>hpo-6</i>	MUC3A	Isoform 2 of Mucin-3A	Mucin	Infection response
<i>irg-1</i>				Infection response
<i>irg-2</i>			DUF1768 domain	Infection response
F49H6.13			Claudin-like	Infection response
F55G11.2			CUB domain protein	Infection response
<i>mul-1</i>			Mucin	Infection response
<i>pcaf-1</i>	PCAF	Histone acetyltransferase	Transcription	Control gene
<i>pcyt-1</i>	PCYT1	Choline-phosphate cytidylyltransferase	PC production	Phospholipid synthesis
<i>pgp-5</i>	ABCB5	ATP-binding cassette 5 isoform 1	Efflux pump	Infection response
<i>pmk-1</i>	MAPK14	Mitogen-activated protein kinase 14	p38 MAP kinase	Pathogenic stress response
<i>pmt-1, pmt-1</i>		phosphocholine methyltransferase	PC production	Phospholipid synthesis
<i>rpb-2</i>	RBP2	RNA Polymerase 2 subunit	Basal transcription	Control gene
<i>sams-1</i>	MAT1A/MAT2A	SAM synthase	SAM synthase	1-carbon cycle
<i>sbp-1</i>	SREBF1	Sterol Response Element binding protein-1	Transactivator	Fatty acid

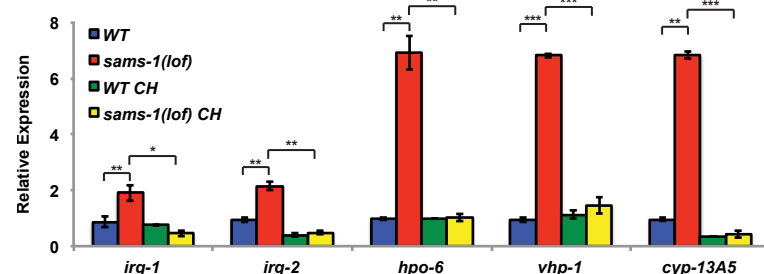
				biosynthesis
<i>set-2</i>	SETD1A/Set1	H3K4 Methyltransferase	Histone modification	Chromatin modifier
<i>set-16</i>	KMT2A/MLL	H3K4 Methyltransferase	Histone modification	Chromatin modifier
<i>sod-3</i>	SOD2	superoxide dismutase	Oxidative stress	Oxidative Stress Response
T24C4.4			Claudin-like	Infection response
<i>taf-1</i>	TAF1	TFIID component	Basal transcription	Control gene
<i>tir-1</i>	SARM1	Sterile alpha and TIR motif- protein	Adaptor protein	Pathogenic stress response
<i>ugt-16</i>	UGT2B7	UDP-glucuronosyltransferase 2B7		Infection response
<i>vhp-1</i>	DUSP16	Dual Specificity Phosphatase	MAP Kinase Phosphatase	Stress response
<i>vit-1</i>		vitellogenin	Yolk transport	Lipid transport
<i>vit-3</i>		vitellogenin	Yolk transport	Lipid transport
Y41C4A.11	COPB2	subunit of the coatomer (COPI) complex	COP I transport	Intracellular transport
Y51B9A.8			CC domain, ShKT domain	Infection response
Y58A7A.5				Infection response

Genes mentioned, with human orthologs and functional classifications for use in our study.

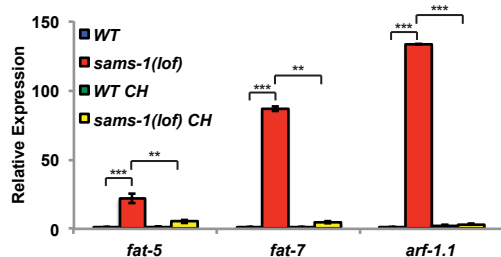
A



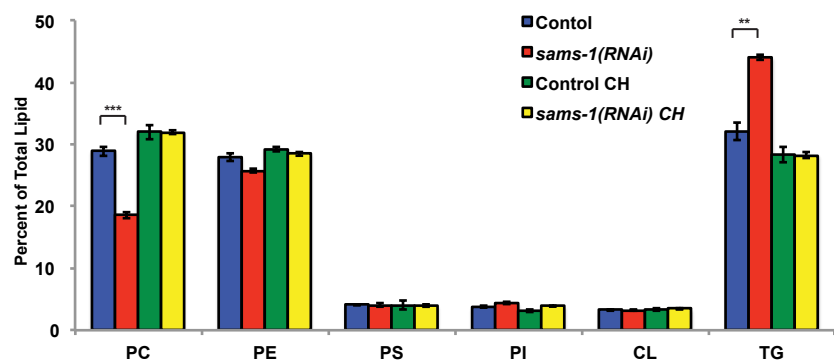
B



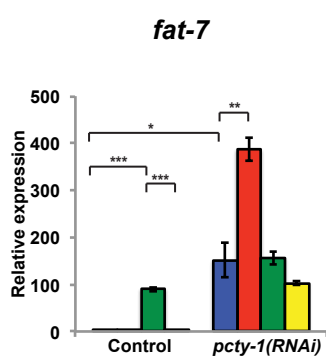
C



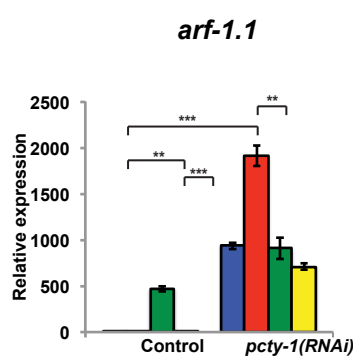
D



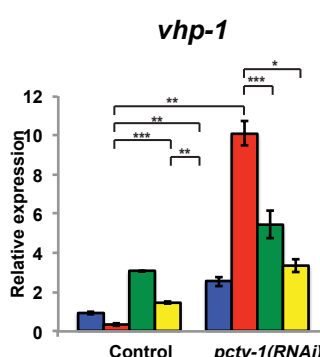
E



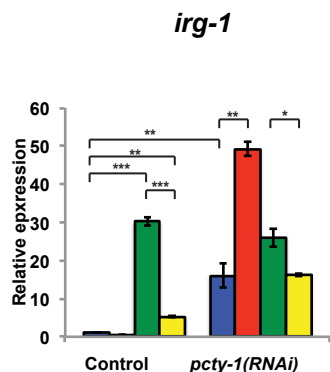
F



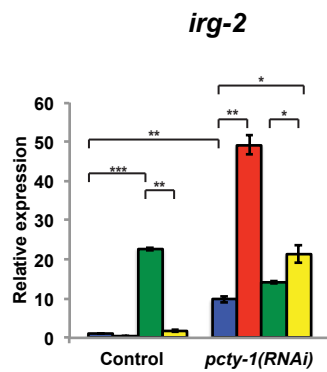
G



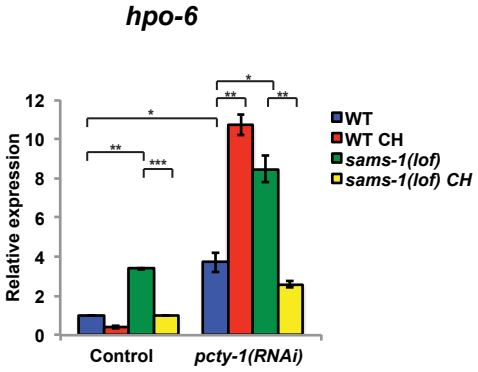
H



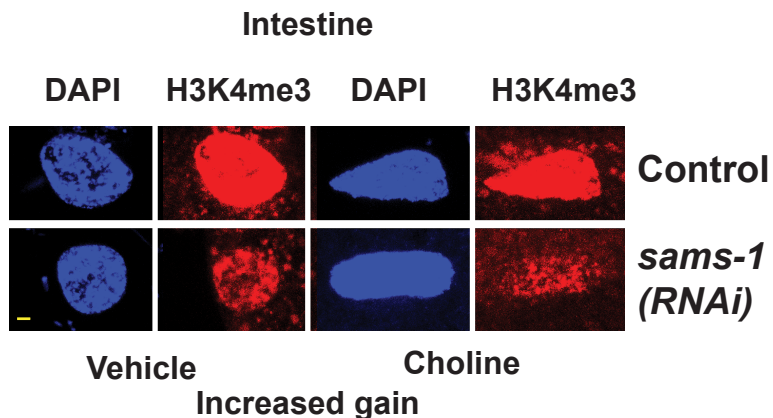
I



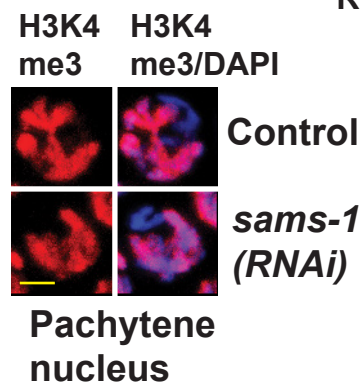
J



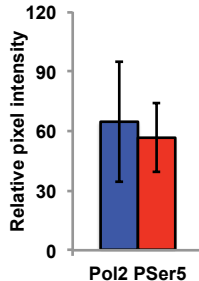
A



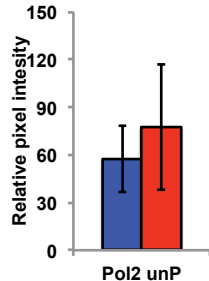
B



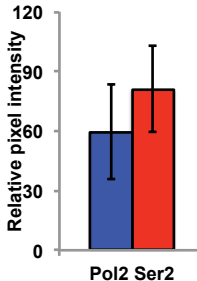
C



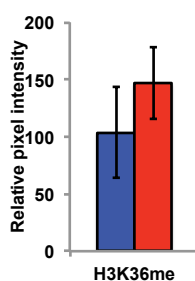
D



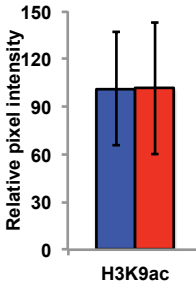
E



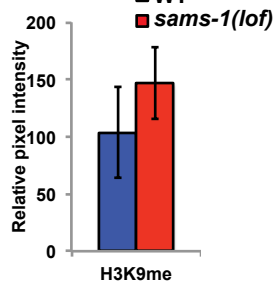
F



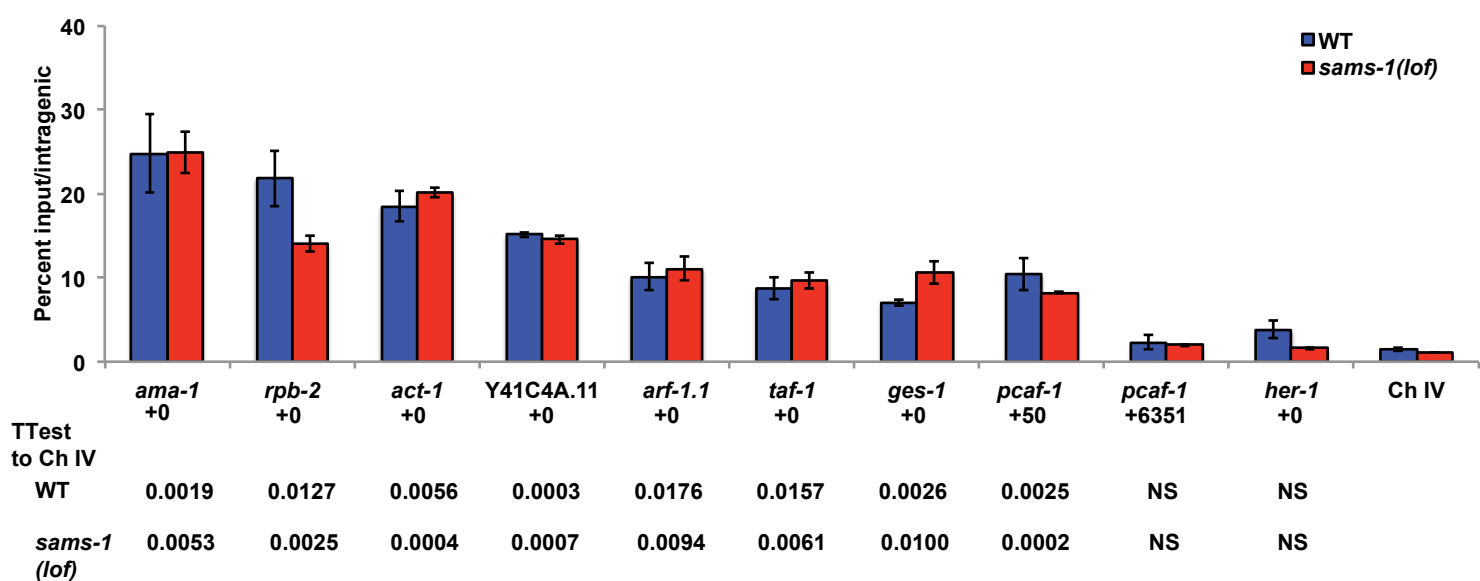
G



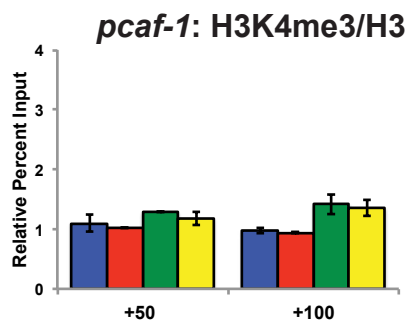
H



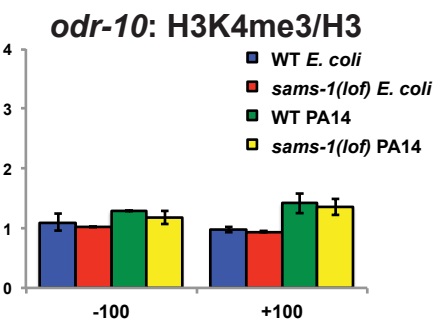
I



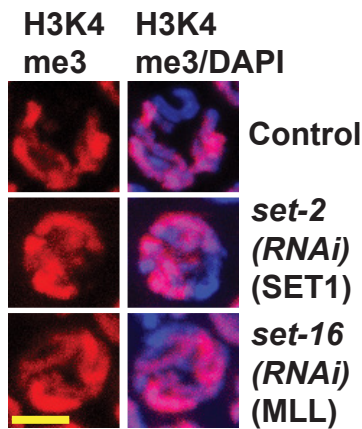
J



K



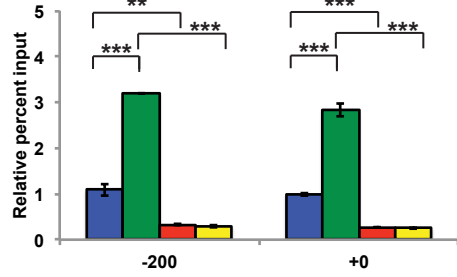
A



Pachytene nucleus

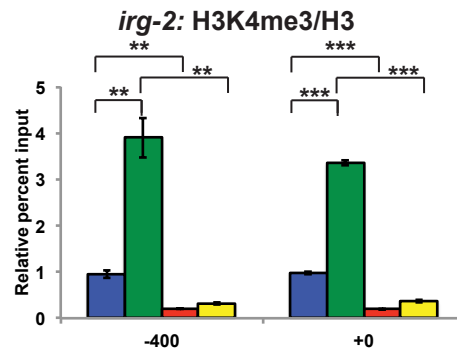
B

irg-1: H3K4me3/H3



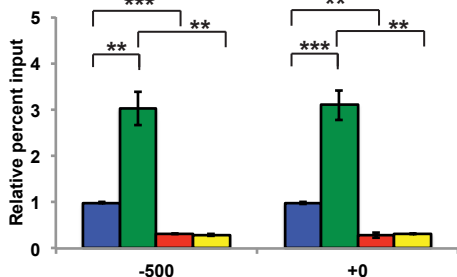
C

irg-2: H3K4me3/H3



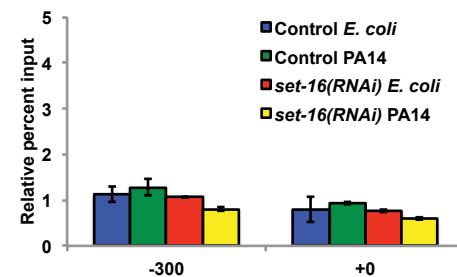
D

hpo-6: H3K4me3/H3

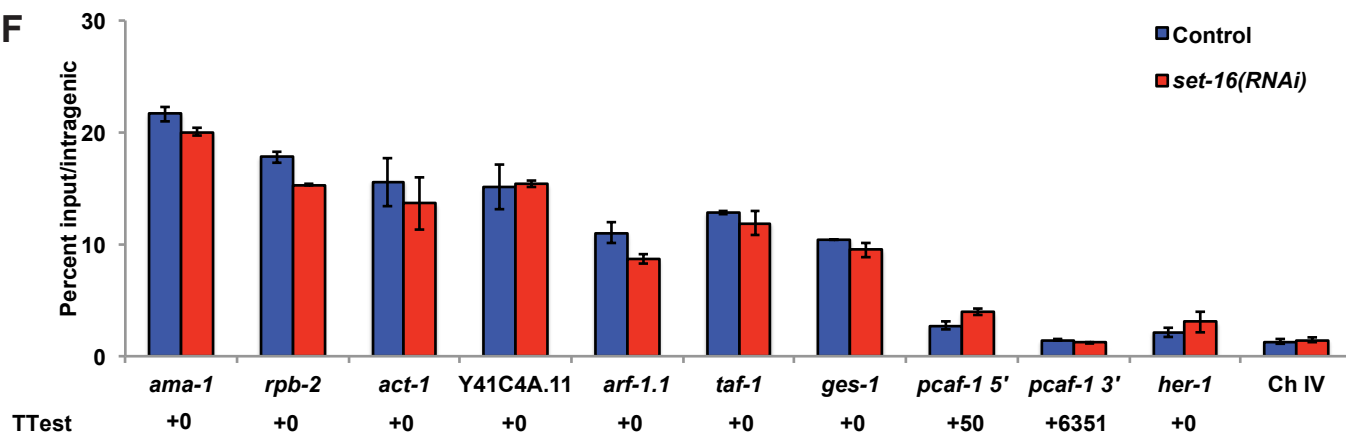


E

sod-3: H3K4me3/H3



F



	+0	+0	+0	+0	+0	+0	+0	+50	+6351	+0	
Control	0.0006	0.0006	0.0116	0.0101	0.0047	0.0003	0.0004	0.0488	NS	NS	
set-16	0.0002	0.0002	0.0180	0.0003	0.0021	0.0057	0.0036	0.0110	NS	NS	

Supplemental Figure Legends

Figure S1. Choline rescues upregulation of lipogenic or innate immune genes in *sams-1(lop)* animals on *E. coli*. (A) Indirect ELISA assay (Artus Biosystems) showing SAM levels normalized to protein concentration in control or *sams-1(RNAi)* animals. qRT-PCR showing expression of genes involved in lipogenesis, or an unrelated, highly expressed gene (**B**) or innate immune genes (**C**) compared between control and choline treated (CH) groups in wild type and *sams-1(lop)* mutants. **D.** GC/MS assays comparing major lipid classes in control and *sams-1(RNAi)* with choline treated samples. PE: phosphatidylethanolamine; PS: phosphatidylserine, PI: phosphatidylinostitol; CL: cardiolipin; TG: triglyceride. RT-PCR comparing choline rescue of *sams-1(RNAi)* with *pcyt-1(RNAi)* for a lipogenic gene (**E**), a highly expressed gene (**F**) or immune function genes (**H-J**). Legend refers to **E-I**. Error bars show standard deviation. Results from Student's T test shown by * <0.05, ** <0.01, *** <0.005.

Figure S2. *sams-1(lop)* mutants fail to accumulate activating histone methylation marks on infection response genes when exposed to *Pseudomonas*. H3K4me3 is diminished in nuclei of intestinal cells (**A**) after *sams-1(RNAi)* and also in choline treated *sams-1(RNAi)*. Yellow bar shows 2 microns. Image is identical to **Figure 6A** with levels increased to visualize staining in *sams-1(RNAi)* nuclei. **B.** Immunofluorescence showing H3K4me3 staining is specific to the transcriptionally active autosomes in pachytene nuclei of *sams-1(RNAi)* germlines. Quantitation of immunoforescence showing an average of pixel intensity over area for 8-12 nuclei per sample for Pol II PSer5 (**C**), Pol II unP (**D**), Pol II Pser2 (**E**), H3K36 (**F**), H3K9ac (**G**) or H3K9me3 (**H**). **I.** Control chromatin immunoprecipitation comparing enrichment of H3K4me3 in control or *sams-1(lop)* animals grown on *E. coli* at the

promoter regions of genes expressed in the intestine and other tissues (*ama-1*, *rpb-2*, *act-1*, *Y41C4A.11*, *arf-1.1*, *taf-1* or *pcaf-1*), an intestinal specific gene (*ges-1*) or a gene that is not expressed in hermaphrodites (*her-1*). Values are relative to an intragenic sequence on chromosome IV. Chromatin immunoprecipitation comparing levels of H3K4me3 around the start site of control genes grown on *E. coli* (OP50) or *Pseudomonas* (PA14) in wild-type (WT) or *sams-1(lof)* mutants for *pcaf-1* (**K**) and *odr-10* (**J**). Input levels are normalized to the WT *E. coli* value on the upstream primer pair. Data from **Figure 6 E-J**, **Figure S2 C, J-K** are from the same representative chromatin immunoprecipitation, separate qPCRs for *pcaf-1* were used in **Figure S2C** and **S2J** to allow comparison to relative gene sets. Error bars show standard deviation. Results from Student's T test shown by * <0.05, ** <0.01, *** <0.005.

Figure S3: set-16/MLL is important for expression of infection response genes upon *Pseudomonas* exposure. **A.** Immunofluorescence showing H3K4me3 staining is specific to the transcriptionally active autosomes in pachytene nuclei after RNAi of *set-2* or *set-16* from hatching to young adulthood. **B.** Control chromatin immunoprecipitation comparing enrichment of H3K4me3 in control or *set-16* animals grown on *E. coli* at the promoter regions of genes expressed in the intestine and other tissues (*ama-1*, *rpb-2*, *act-1*, *Y41C4A.11*, *arf-1.1*, *taf-1* or *pcaf-1*), an intestinal specific gene (*ges-1*) or a gene that is not expressed in hermaphrodites (*her-1*). Values are relative to an intragenic sequence on Chromosome IV. Representative chromatin immunoprecipitations comparing induction of infection response genes (**C-E**) and a control gene (**F**) in response to PA14 after control or *set-16 RNAi*. Error bars show standard deviation. Results from Student's T test shown by * <0.05, ** <0.01, *** <0.005.

Supplemental Experimental Procedure

SAM measurements: 1 gram of young adult *C. elegans* were frozen liquid nitrogen, then ground to a fine powder in a -80 degree mortar. After solubilization in 2 milliliters of phospho-buffered saline, extracts were sheared in a Dounce homogenizer with pestle B before sonication for 2-5 20 second bursts. Lysates were cleared, then 30 microliters was used a SAM measurement ELISA kit (Artus Bioscience).